Journal of Building Engineering 66 (2023) 105888

Contents lists available at ScienceDirect

Journal of Building Engineering

journal homepage: www.elsevier.com/locate/jobe

Jute fiber-reinforced mortars: mechanical response and thermal performance

Arnas Majumder [a], Flavio Stochino [b,*], Andrea Frattolillo [b], Monica Valdes [b], Geminiano Mancusi [a], Enzo Martinelli [a]

[a] Department of Civil Engineering, University of Salerno, via Giovanni Paolo II n.132, 84084, Fisciano, SA, Italy
[b] Department of Civil Environmental Engineering and Architecture, University of Cagliari, via Marengo 2, 09123, Cagliari, CA, Italy

A B S T R A C T

Enhancing energy efficiency and structural capacity are the main objectives of masonry retrofitting. However, a combined enhancement of both aspects is hardly achievable, as they are related to the relevant geometric and physical parameters in a somewhat "competitive" fashion. Therefore, the main focus of this research is to achieve the dual positive effect by improving both thermal insulation properties and structural behavior of composite building materials, also with an eye to sustainability. In this context, jute fibers composite mortars were fabricated by using three different fiber lengths (5 mm,10 mm and 30 mm) and four different fiber percentages (0.5%,1%,1.5% and 2%) with respect to the mortar masses. Unreinforced mortar samples showed fragile collapse during the flexural and compression (with hour-glass shape) tests. Whereas the fiber reinforced mortar samples exhibited higher ductility and strain energy but lower strength. These composite samples present also higher thermal resistance as the fiber percentage increases. Samples with longer fibers (30 mm, in all fiber percentage category) can dissipate more mechanical energy, whereas the samples with shorter fibers (5 mm, in all fiber percentage category) have lower thermal conductivity values, which leads to improving the insulation capacity of the composite samples.

1. Introduction

A large portion of the existing built stocks is significantly vulnerable to natural disasters (earthquakes, floods etc.) [1], whereas new constructions need to follow the energy efficiency [2] and seismic [3] standards. The European Union (EU) aims to (i) reduce the greenhouse gas emissions of 40% (from 1990 levels), (ii) have the renewable energy production share of 32%, and (iii) improve the efficient use of energy of 32.5% by 2030 as stated in the Paris agreement [4,5]. To accomplish these goals, EU also has adopted the "near Zero Energy Building" (nZEB) regulation to realize energy efficient buildings [6]. EU has also implemented Eurocode 8 to improve the seismic performance of buildings [3,6].

According to the World Economic Forum (WEF), the quality of life (including happiness) could be judged with respect to five parameters: job, wellbeing, environment, fairness and health [7]. Approximately 39.44% of the total World population still live in rural villages but this number is higher (i.e., between 50% and 86.65%) in 63 counties out of 196 [8]. As reported by the United Nations Development Program (UNDP), 17 in 100 people do not have access to proper shelter and 33 people out of every 100 people don't have access to electricity [9]. Therefore, it is evident that a big portion of the World population is still deprived of basic goods.

However, environmental awareness has gained more attention in the last years, and many Countries are committed towards the sustainable development goals presented by the United Nations (UN) [10]. In this context, it is worth to highlight that living in eco-friendly healthy houses could lead to wellbeing among population, fairness, equality and happiness. Therefore, it would not only

* Corresponding author.
E-mail addresses: amajumder@unisa.it (A. Majumder), fstochino@unica.it (F. Stochino), andrea.frattolillo@unica.it (A. Frattolillo), m.valdes@unica.it (M. Valdes), g.mancusi@unisa.it (G. Mancusi), e.martinelli@unisa.it (E. Martinelli).

https://doi.org/10.1016/j.jobe.2023.105888
Received 16 August 2022; Received in revised form 20 December 2022; Accepted 12 January 2023
Available online 14 January 2023
2352-7102/© 2023 The Authors. Published by Elsevier Ltd. This is an open access article under the CC BY license (http://creativecommons.org/licenses/by/4.0/).

create a sustainable society with smart cities but also would give birth to smarter villages.

For these reasons sustainable and integrated (thermal and structural) design [11–13] nowadays represents an important research field.

The thermal behaviors of cementitious composites [14], fiber reinforced concrete [15,16] foamed concretes [17] have been investigated in literature highlighting that density/porosity and moisture content strongly influences their thermal conductivity. Many standard references on mortar thermal performances are present in Ref. [18].

Actually, new composite construction materials can be designed to have good thermal insulating property and good structural behavior. This can be obtained using conventional or recycled construction products enhanced with natural materials, like locally available and cheap fibers.

The use of fibers in construction is getting more and more common, and both man-made and natural fibers are widely used for various purposes [19].

Due to high strength and durability [20], the man-made carbon [21–23], glass [24–26] and basalt [27–29] fibers are mainly used for structural retrofitting in Fiber Reinforced Polymers (FRP) configuration. Also carbon, glass and basalt [30,31], as well as steel [31–33] fibers are used in Textile Reinforced Mortar (TRM).

In order to improve sustainability, recyclability and reduce the carbon footprint and production cost of construction materials, scientists and researchers are working on the development of natural fiber [34], TRM [35–37] and composite building materials [38–42] and their mechanical properties are being studied.

While highlighting the studies done on the thermal property of composite building materials, it is important to mention that the natural fibers are mainly used in raw form or mixed with other nature materials like clay [43,44], lime putty [38], opus signinum [43], potato starch [45] etc. In other case the fibers are mainly fused with polyester or bicomponent to fabricate thermal insulating materials.

The pros and cons of natural fibers are reported in Ref. [19]; based on the most recent data [46], natural fibers (flax, hemp, jute or kenaf) have 78%–79.4% lower carbon footprint, when compared with glass or mineral fibers.

In this context, a promising new idea is the development of hybrid fibers composite in which both natural and man-made fibers are applied together [47].

Jute fibers are gaining importance in the building and construction field. It is interesting to highlight that each and every part of the jute plant can be used for various purposes like food and medicinal (leaves), industrial and household (fibers) and fuel (Jute stalks). Jute fiber accounts for approximately 7% of the total natural fiber production [48]. When compared with man-made and mineral fibers and their products, jute fibers and its products require lower-energy for the production process and less hazards during manufacturing [49]. Additionally, its cultivation improves the fertility of the soil, purify the air by absorbing CO_2 and emitting O_2 [50]. The jute fiber is, cheap, recyclable, whereas its strength and insulating capacity [51] also make it an attractive and competitive construction material. Like all other natural fibers, jute fibers inherit some disadvantages, like the detrimental effects of water that induces strength decrease and moisture absorbability increase [51].

Various studies investigate the use jute fibers in concrete retrofitting [52–54], Jute-FRP [33], recycled jute fiber (collected from packaging bag) insulating materials [43,45], jute fiber products (threads and diatons) [55], jute composite mortar [50,56,57], recycled jute net fiber composite mortars [58], jute epoxy composites [59], jute fiber crude earth bricks [60], jute fiber burnt bricks [61] etc.

The thermo-mechanical performance of the composite mortar systems fabricated with natural fibers (like date palm, hemp, sheep wool and oil palm fibers) have been studied [62–65]. However, most of the researchers mostly focus on evaluating physical and/or mechanical properties or thermal behavior. The combined behavior, i.e., mechanical and thermal properties of the jute fiber composite materials has not yet been studied deeply.

Therefore, this paper aims to investigate the dual positive effect of the jute fiber on composite mortar system. Both the mechanical and the thermal properties will be analyzed in order to find the optimal composite material.

After this brief introduction the paper is organized as follows: Section 2 describes the material properties, mortar and composite mortar samples preparation and the test procedures. While in Section 3 the results obtained for the normal and composite mortars (for various mix design with different fiber lengths, fiber percentages (with respect to the dry mortar) and water amount) are reported, and their mechanical and thermal properties are also described. Some conclusive remarks are pointed out in Section 4.

2. Materials and methods

Fig. 1 describes the underlying methodology for the present research.

2.1. Materials

2.1.1. Jute raw fibers

The raw fibers have been collected from West Bengal, India (Fig. 2). These fibers are of Bangla Tosha - Corchorus olitorius (golden shine) origin and are in average 3–4 m long. The physical and mechanical properties of these fibers and their cutting process can be found in Ref. [55]. The average mechanical properties of the raw fibers are the following: strain energy 0.77 Nmm, tensile strength 215.11 MPa, maximum axial strain 0.0131, elastic modulus 16.97 GPa.

In this work, three jute fiber lengths (30 mm, 10 mm and 5 mm) (Fig. 3) were considered for the preparation of the composite mortars.

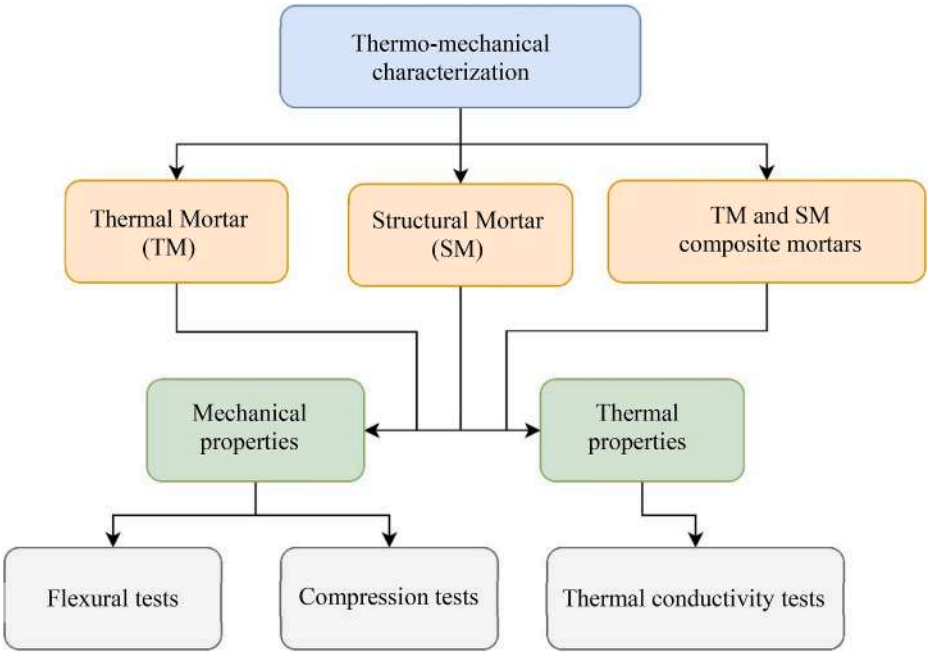

Fig. 1. Experimental procedures.

Fig. 2. Raw jute fiber.

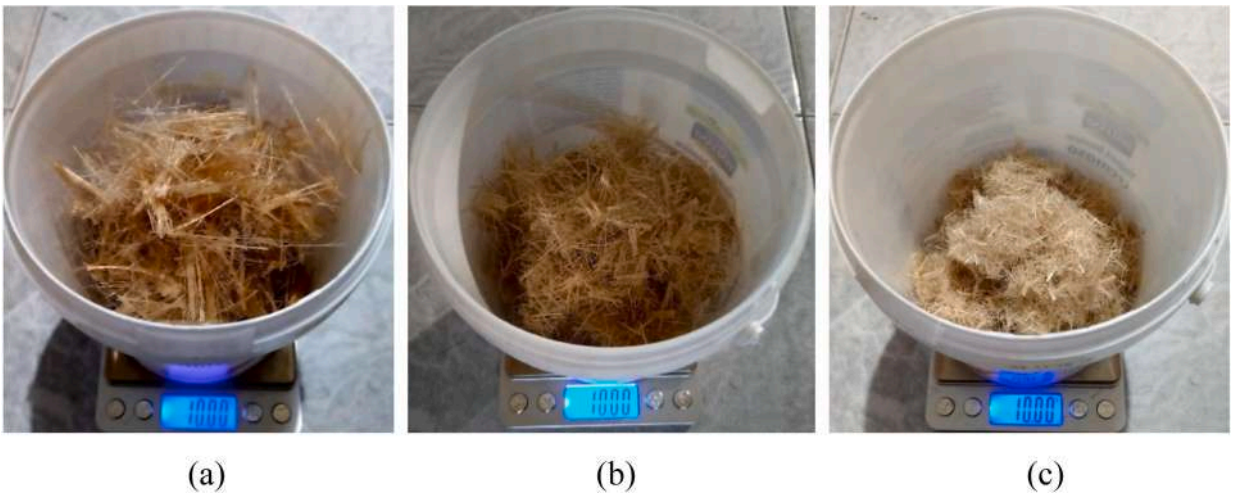

Fig. 3. 10 gs of (a) 30 mm, (b) 10 mm and (c) 5 mm chopped jute fibers.

2.1.2. Mortars

Two types of commercial mortars were used, namely a lime based Thermal Mortar (TM) and cement-based Structural Mortar (SM). The TM is a thermo-dehumidifying plaster certified R and T/CSII (EN 998-1 [66]) characterized by a dry density of 750 kg/m^3. In the TM mix there are recycled aggregates with the grading curve of 0–1.4 mm, able to give better thermal properties to the final mortar. The SM is a premixed mortar for masonry with hydraulic binders and selected aggregates. Its compressive strength is 10 MPa, while its shear strength is 0.15 MPa with a dry density of 1545 kg/m^3.

2.2. Test procedure

2.2.1. Mortars and jute fiber composite mortars preparation

First of all, the thermal and structural mortar samples grouts were prepared following EN 1015-2 [67] and their workability were verified through shaking table tests at fresh state, as prescribed in EN 1015-3 [68]. The workability tests values of the first thermal and mechanical mortars were used as a benchmark for the composite mixtures. Also, while preparing the composite-mortar samples, the EN 1015-2 and EN 1015-3 standards have been followed. The jute fiber composite-mortars were fabricated with three different fiber lengths 30 mm, 10 mm and 5 mm (see Fig. 3) and using four different percentages (0.5%,1%, 1.5% and 2%) with respect to the dry mortar mass. In this phase of the experimental campaign, the amount of water was different for each mix in order to take into account the fiber absorption capabilities already studied in Ref. [55]. For this reason, in Table 1 the details of the mix design have been reported.

For identification purposes, the samples are labelled as reported in Table 2. The labels start with M and MS, respectively representing the thermal and structural mortars. Thereafter, there is the casting number (x), the mortar sample type with fiber (F), the fiber percentage (0.5%, 1.0%, 1.5% and 2.0%), the fiber length (30 mm, 10 mm and 5 mm), the serial of the mold (M) number (y) and finally the sample (S) serial number (z). For example: MxF0.5(10)MySz denotes the sample number z, realized with thermal mortar M, using the mold x, with fiber percentage 0.5% and fiber length 10 mm.

Two molds were used to prepare 6 samples (160 mm × 40 mm × 40 mm) for the mechanical test. Moreover, another two molds were used to prepare 2 samples (160 mm × 140 mm × 40 mm) for thermal conductivity tests.

While preparing the composite samples, the fibers were initially mixed with the dry mortar for 30 s inside the mixture (Fig. 4) without any water. Thereafter, an appropriate amount of water was added (Table 1) and mixed for 7 min. The amount of water, necessary for the mixture was determined through the water absorption test (for more details see Ref. [55]).

After mixing, the shaking table test was performed to evaluate the mortar workability.

During this process a hollow conical bronze mold was used to cast the test specimens on the shaking table. The mortar was put

Table 1
Mix design for the normal mortar and composite mortar mixtures.

	Thermal Mortar	Jute Fiber	Water		Structural Mortar	Jute Fiber	Water
M (No fiber)	75.000%	0.000%	25.000%	MS (No fiber)	84.753%	0.000%	15.247%
MF0.5(5)	70.764%	0.356%	28.880%	MSF0.5(5)	82.039%	0.414%	17.547%
MF0.5(10)	71.186%	0.358%	28.457%	MSF0.5(10)	82.295%	0.415%	17.290%
MF0.5(30)	72.134%	0.362%	27.503%	MSF0.5(30)	82.865%	0.418%	16.716%
MF1(5)	66.969%	0.676%	32.355%	MSF1(5)	79.477%	0.803%	19.719%
MF1(10)	66.825%	0.702%	32.473%	MSF1(10)	79.962%	0.808%	19.230%
MF1(30)	69.452%	0.701%	29.846%	MSF1(30)	81.059%	0.819%	18.122%
MF1.5(5)	63.922%	0.976%	35.102%	MSF1.5(5)	77.340%	1.178%	21.482%
MF1.5(10)	64.925%	0.991%	34.084%	MSF1.5(10)	78.207%	1.191%	20.602%
MF1.5(30)	67.251%	1.027%	31.723%	MSF1.5(30)	79.497%	1.211%	19.293%
MF2(5)	60.865%	1.242%	37.893%	MSF2(5)	74.784%	1.526%	23.689%
MF2(10)	62.088%	1.267%	36.645%	MSF2(10)	75.652%	1.544%	22.804%
MF2(30)	64.968%	1.326%	33.706%	MSF2(30)	77.635%	1.584%	20.781%

Table 2
Composite mortar preparing scheme.

		Fiber length		
		30 mm	10 mm	5 mm
Fiber percentage	0.5%	MxF0.5(30)MySz MSxF0.5(30)MySz	MxF0.5(10)MySz MSxF0.5(10)MySz	MxF0.5(5)MySz MSxF0.5(5)MySz
	1.0%	MxF1(30)MySz MSxF1(30)MySz	MxF1(10)MySz MSxF1(10)MySz	MxF1(5)MySz MSxF1(5)MySz
	1.5%	MxF1.5(30)MySz MSxF1.5(30)MySz	MxF1.5(10)MySz MSxF1.5(10)MySz	MxF1.5(5)MySz MSxF1.5(5)MySz
	2.0%	MxF2(30)MySz MSxF2(30)MySz	MxF2(10)MySz MSxF2(10)MySz	MxF2(5)MySz MSxF2(5)MySz

*M = thermal mortar; MS = structural mortar; x = mortar casting sequence; y = number of molds; z = sample number.

Raw fibers: 30mm, 10mm and 5mm + Fiber percentages 0.5% or 1.0%, 1.5% or 2.0%
+Water amount as necessary, based on the calculation.

Jute +Mortar (Mixed for 30 secs).

Jute +Mortar +water (Mixed for 7 mins).

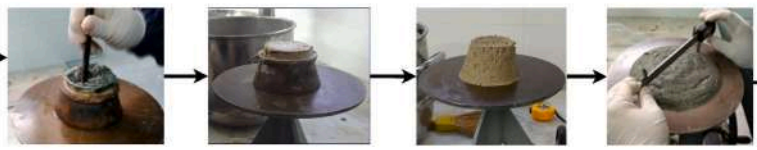

Shaking table test.

1 Sample (160 x 140 x 40 mm)
for thermal conductivity test.

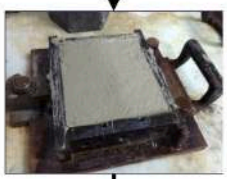

3 Samples (160 x 40 x 40 mm)
for mechanical conductivity.

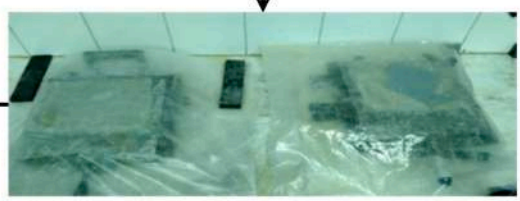

Initial drying period in molds and inside plastic bags from the casting day to 3rd day.

Intermediate drying period inside
plastic bag from 3rd day to 8th day.

Final drying period from 8th
day to 28th day.

Fig. 4. Jute fiber composite mortar preparation.

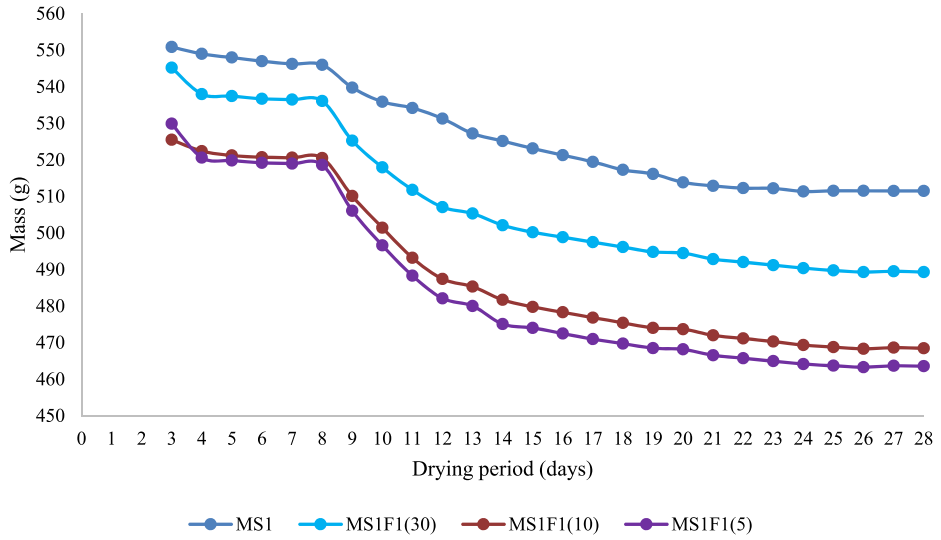

Fig. 5. A typical example of samples drying period of a structural mortar and composite mortars with different fiber lengths (30 mm, 10 mm and 5 mm) and 1% of jute fiber (with respect to the mortar dry mass).

inside this conical mold and 15 strokes were applied to the half-filled grout, to distribute the mixture uniformly around the bottom of the mold. Thereafter, another portion of the mixture was put in to completely fill the mold. Then, 15 more strokes were applied, and then the extra materials were removed from the top. Then the mold was removed vertically, and the table was shaken for 15 times by rotating a lever attached to the table at a frequency of 1 s/rotation.

After the first shaking table test, the orthogonal diameters of the spread normal-mortars or composite mortars were measured with a digital vernier caliper. An average±10% variation range between two consecutive tests assured the mixtures composition correctness. Otherwise, the normal-mortar or composite-mortars were re-prepared and the shaking table tests were re-conducted. While preparing the samples inside the molds, 25 strokes were applied for each mechanical samples (160 mm × 40 mm × 40 mm), while 75 strokes were applied for each thermal sample (160 mm × 140 mm × 40 mm). This was done to remove the trapped air in the samples.

The EN 1015-11 standard [69] has been followed for samples curing. The curing period consists of a total of 28 days from the day of casting. After casting, all the samples were kept inside airtight plastic bags and left inside molds for first two days after casting date. On third day samples were taken out from the respective first plastic bag and mold and re-put inside another plastic bag for 5 days. This controlled drying period corresponds 2nd to 8th day in Figs. 5 and 6 reporting the samples mass variation during the drying period.

On the 8th day after casting, all the samples were extracted from plastic bags and placed in a room with ambient temperature 25 °C and relative humidity 65%.

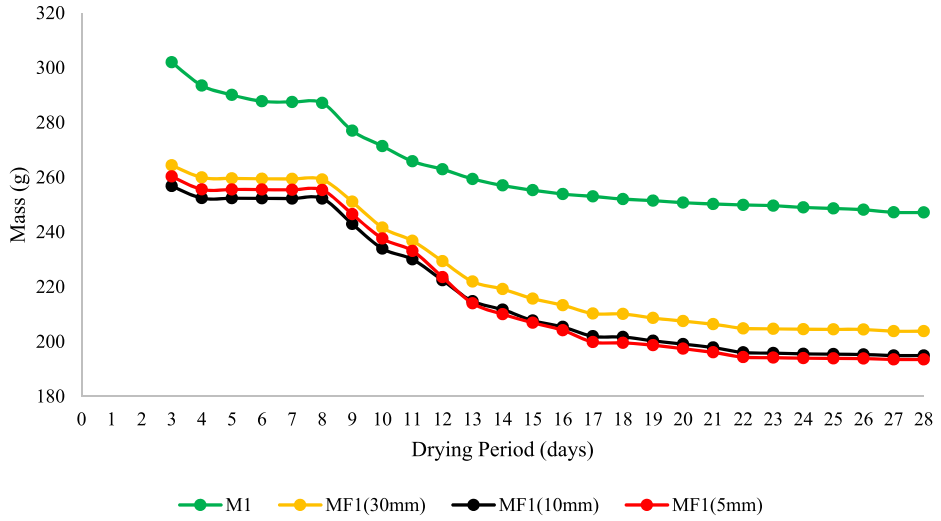

Fig. 6. A typical example of samples drying period of a thermal mortar and composite mortars with different fiber lengths (30 mm, 10 mm and 5 mm) and 1% of jute fiber (with respect to the mortar dry mass).

2.2.1.1. Recycled jute fiber composite mortar. A set of jute fibers were also collected from the jute net, and class 1 mm threads used for the retrofitting of masonry walls. A total of 3.5 (kg) of jute threads have been used for preparing the net-fabrics, of which 3.5% came out as waste product. These scraps residual thread fibers have been used for the preparation of the Recycled Jute Fiber Composite Mortar (RJFCM).

In this case, the recycled aggregates have been separated from the original thermal mortar, using a vibrating screen machine and the residual jute thread fibers, collected during net preparation, were used as insulating and retrofitting material.

So, 6.5% with respect to the mortar dry mass, of recycled jute thread fiber have been used in the mixture.

Approximately 39% of water with respect to the total composite mortar mixture (mortar without recycled aggregates + fibers) mass has been used (Fig. 7).

2.3. Alternative mixes

Other three types of jute fiber composite samples and their mechanical and thermal behaviors have been studied:

Case 1. Same Average Water (SAW) was used for all the 30 mm,10 mm and 5 mm fibers and the percentage of jute fibers 0.5% and 1.0% (with respect to the thermal and structural mortar mass) have been used.

Case 2. the percentage of jute fiber is 1.0% with respect to the thermal mortar mass without the pre-existing recycled aggregates (Fig. 7b). Here too, the SAW has been used.

The choice of 1% jute fibers can be based on the following considerations:

- A balance between these integrated properties obtained in the previous measurements;
- Acceptability of these samples as incombustible composites therefore the presence of fiber should be lower and equal to 1%, according to EN 13501-1 [70].

Case 3. In this case, the recycled jute thread fiber (class 1 mm) collected during net fabrication, has been used (Fig. 7a) with respect to the thermal mass without pre-existing recycled aggregates (Fig. 7b).

In Case 3, samples have been fabricated with 6.5% of recycled Net Fiber (NF) considering:

- Feasibility of substitution of recycled aggregates with recycled jute fibers;
- Acceptability of the mortar workability;

(a)

(b)

Fig. 7. (a) Recycled jute fiber, thermal mortar without recycled aggregates and (b) separated recycled aggregates.

Fig. 8. Composite (a) TM and (b) SM samples with 1% fiber with respectto the dry mortar mass, of fiber lengths 30 mm, 10 mm and 5 mm.

- Use of sustainable and ecofriendly materials;
- To achieve the overall sustainability of the whole project.

2.4. Mechanical properties tests

The mechanical properties of both thermal and structural unreinforced mortar samples and fiber-reinforced mortar samples (Fig. 8 a and b) were evaluated through flexural and compression tests, on the 28th day from the casting date.

Before conducting the tests, mass and dimensions of each sample were measured, and later these values were used while calculating flexural and compressive values. The three-point bending flexural test was conducted according to EN 1015-11 [69], using a universal displacement-controlled machine: Metrocom-1 (Fig. 9), characterized by a maximum load capacity of max. 4.9 kN and sensibility of 0.02 kN.

Fig. 9. Flexural strength Test: Sample M1F0.5(30) M1S2.

(a) (b)

Fig. 10. (a) Thermal mortars and (b) structural mortars without fiber and with 2% of fiber (with respect to the dry mortar mass) with 30 mm, 10 mm and 5 mm of fiber length, respectively.

Fig. 11. Compression strength test: sample M1F0.5(30) M1S2.

The three-points flexural tests were executed on prismatic specimens (dimensions 160mm × 40mm × 40mm) with displacement rate of 1.5 mm/min. The applied force was measured by using a load cell of class 1 (Fig. 9), having a maximum capacity of 5 tons and nominal sensibility of 2 mV/V. A Linear Variable Displacement Transducer (Fig. 9) was used to measure the displacement, its specifications are: max. measuring length 50 mm, nominal sensitivity 2 mV/V and linearity -<0.10% of span.

After the flexural test, the remaining two parts of the tested specimens (Fig. 10) have been subjected to the compression tests (Fig. 11). These tests were conducted using a universal load-controlled machine Metrocom-2 that has a load capacity of 100 kN.

2.5. Thermal properties tests

A heat flow meter instrument was used to evaluate the thermal properties of the mortar (without fiber) and the composite mortar samples. The measurements were conducted following ISO 8301 [71] and EN 1946-3 [72], using the heat flow meter measuring device TAURUS TCA 300 (for simplicity hereafter it will be called only TAURUS), see Fig. 12.

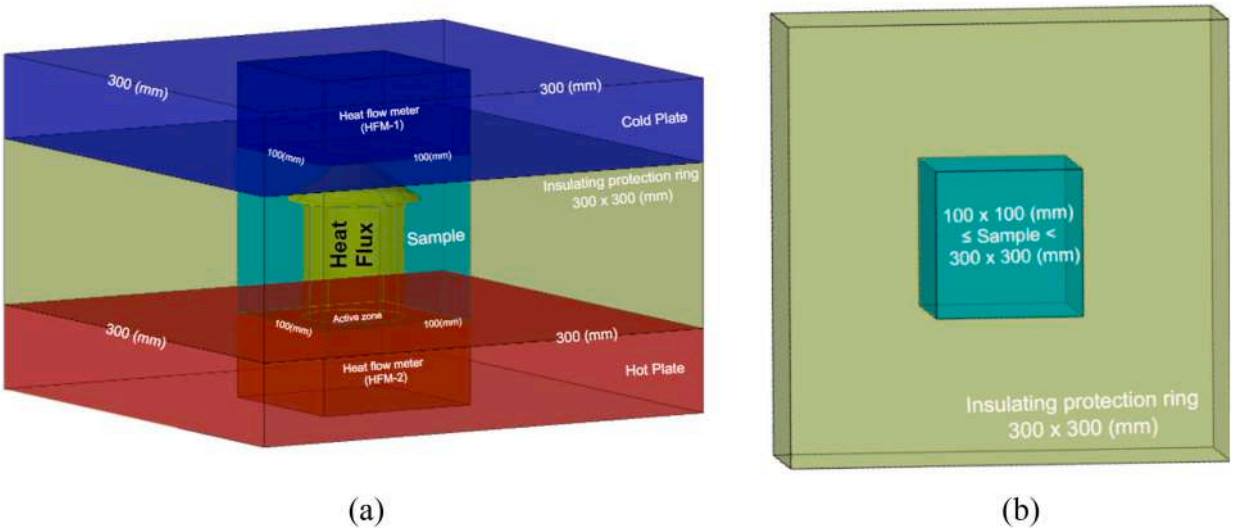

Fig. 12. (a) Schematic diagram of heat flow meter (TAURUS); (b) In general insulating protection materials like EPS or sheep wool must be used in the case with sample 100 × 100 (mm^2)≤ Sample<300 × 300 (mm^2).

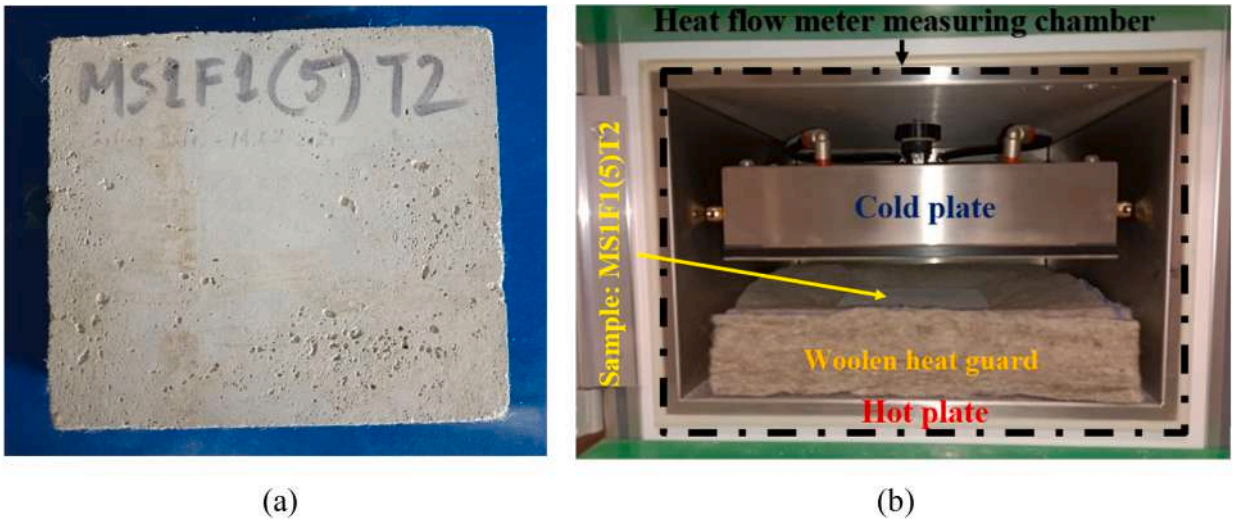

Fig. 13. (a) Sample MS1F1(5)T2 (160 × 140 mm^2) used for the TC test and (b) Sample placed inside the measuring chamber.

A total of 5 measurements were conducted on each sample, out of which four (10th, 15th, 22nd and 28th day) were taken during the natural drying period and the last once the drying process is complete. This was done to measure the change in the thermal conductivity with the reduction in water/humidity content in the tested samples. The samples were dried in an oven at constant temperature of 50 °C according to EN 12667 [73]. The forced oven drying time varied depending on the moisture contain, ranging from 5 to 14 days. While drying in the oven, the mass of the samples was daily monitored, until two successive measurements were equal (with a margin of error of ± 0.1 g). When constant weight for samples was achieved, the samples were wrapped and kept inside airtight plastic bags and taken out only before putting inside so-called TAURUS for measurements. Samples masses were also measured before and after every thermal conductivity test. All sample mass measurements were carried out in the laboratory where temperature is controlled at 25 ± 3 °C and relative humidity is 60 ± 10%.

TAURUS is equipped with hot and cold plates (Fig. 12a). The instrument has a total workable surface area of 300 mm × 300 mm, whereas both plates active zone has a surface area of 100 mm × 100 mm and is situated at the center of the plates. These active measuring zones are equipped with one heat flux sensor per plate arranged symmetrically in this area. Protective zones are located outside the plates active zone. The intermediate sampling time was set at 1 min; therefore, the instrument provides the calculated value of thermal conductivity at an interval of each minute for 300 min (set as total measuring time period). According to EN 12939 [74] the sample mean temperatures were chosen to be equal to 10 °C, 20 °C and 30 °C, with the plate's temperature difference selected to be

10 °C. All the thermal samples have the upper and lower surface areas equal to 160 × 140 mm^2 (as like, Fig. 13a); with thickness equal to 40 mm. Being greater than the active zone surface areas 100 × 100 mm^2 but being smaller than total plate areas 300 × 300 mm^2, a protective woolen insulating ring was used (Fig. 13b) around each sample. This was done to avoid the heat losses along around the sample's edges and thus ensuring a uniform heat flux passing through the sample, under observation. The sheep wool was chosen as it has one of the lowest thermal conductivity values among other thermo-insulating materials, which is approximately around 0.0378 W/mK. The heat fluxes were measured and the thermal conductivity λ value was calculated by enforcing its definition presented in Eqn 1:

$$\lambda = \dot{Q}\,\frac{S}{A(t_H - t_C)} \tag{1}$$

where $\dot{Q}$ is the heat flux in W/m^2; s is the sample thickness in m, t_H is the hot plate temperature in °C; t_C is the cold plate temperature in °C and A is the active zone surface area of the sample under test.

3. Results and discussion

3.1. Physical properties and observations

Workability of the mortars was evaluated through the shaking table test at fresh state.

The mortars workability threshold was judged by comparing the average diameter of each mortar sample with the average diameters (used as reference value) of the normal-thermal mortar (M) and normal structural mortars (MS) spreading diameters, 151.65 mm and 163.64 mm, respectively. The workability limit state is fulfilled if the percentage difference between the spreading diameters is below 10%. The accepted shaking table tests values are listed in Table 3 (thermal mortars) and Table 4 (structural mortars).

Table 3
Shaking table tests: Jute fiber thermal composite mortars.

Values with respect to±10% of the thermal mortar (M)							
MF0.5(5)	0.70%	MF1(5)	8.27%	MF1.5(5)	9.55%	MF2(5)	9.18%
MF0.5(10)	9.9%	MF1(10)	4.12%	MF1.5(10)	6.88%	MF2(10)	1.66%
MF0.5(30)	10.0%	MF1(30)	3.09%	MF1.5(30)	3.08%	MF2(30)	6.03%

Table 4
Shaking table tests: Jute fiber structural composite mortars.

Values with respect to±10% of the structural mortar (MS)							
MSF0.5(5)	0.50%	MSF1(5)	3.65%	MSF1.5(5)	2.33%	MSF2(5)	9.85%
MSF0.5(10)	3.17%	MSF1(10)	1.17%	MSF1.5(10)	5.50%	MSF2(10)	9.10%
MSF0.5(30)	2.58%	MSF1(30)	5.78%	MSF1.5(30)	6.30%	MSF2(30)	9.90%

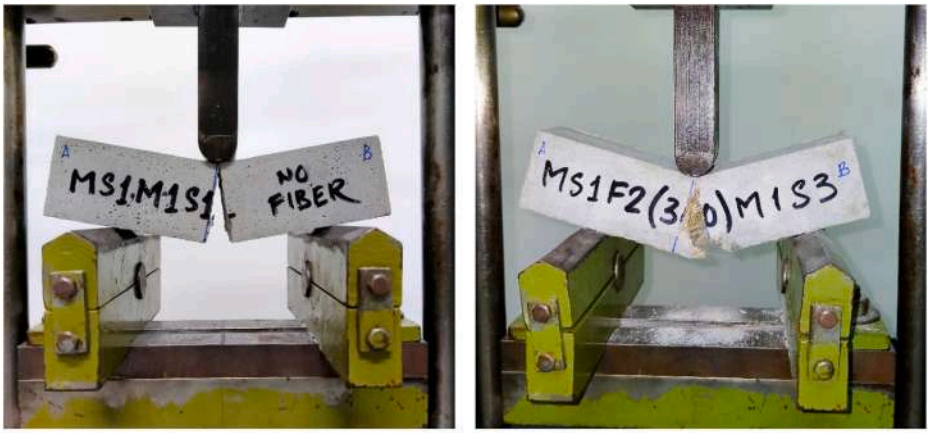

Fig. 14. Samples (a) MS1M1S1 without fiber and (b) MS1F2(30)M1S3 with 2% fiber (30 mm) with respect to dry mortar mass.

3.2. Mechanical properties and observations

The samples mechanical performances were assessed through flexural and compression tests. Overall, 240 mortar samples have been used for the flexural tests. Moreover, 480 samples have been used for the compression tests.

3.2.1. Flexural test

Fig. 14 a shows a typical collapse of the structural mortar sample without fiber, where the sample breaks immediately after reaching the ultimate flexural strength. The complete collapse has been recorded for all types of samples (thermal and structural) without fiber.

Table 5
Thermal mortar and composite mortars flexural test properties.

	Deflection max. (d)		Strain energy		Flexural stress (σ)		Flexural strain (ε)		Moment of inertia (I)	
	Mean	Co.V	Mean	Co.V	Mean	Co.V	Mean	Co.V	Mean	Co.V
	mm	%	kNmm	%	MPa	%		%	mm^4	%
M (no-fiber)	0.603	9.403	0.186	29.723	1.156	6.487	0.013	9.701	229219.484	1.051
MF0.5(5)	0.483	19.653	0.176	20.935	0.978	7.852	0.010	19.084	238651.134	3.969
MF0.5(10)	0.840	12.135	0.200	20.434	0.919	6.014	0.018	12.188	236889.402	2.025
MF0.5(30)	0.839	44.548	0.538	48.984	1.214	2.877	0.017	44.838	232294.789	2.483
MF1(5)	0.137	26.334	0.020	19.551	0.429	10.245	0.003	35.624	235590.026	3.523
MF1(10)	0.996	28.624	0.229	25.624	0.662	7.264	0.021	29.221	243081.565	2.553
MF1(30)	0.666	40.240	0.563	42.170	0.634	8.907	0.015	37.575	239004.001	0.885
MF1.5(5)	0.549	31.646	0.121	23.748	0.505	5.091	0.011	31.299	238988.136	1.458
MF1.5(10)	0.611	26.956	0.272	7.662	0.490	10.212	0.013	27.151	242856.595	2.158
MF1(30)	0.613	45.588	0.543	51.208	0.563	16.549	0.013	45.218	259554.012	2.594
MF2(5)	0.512	28.570	0.054	38.430	0.283	29.895	0.011	28.672	235421.779	0.714
MF2(10)	0.908	44.539	0.187	30.480	0.373	7.695	0.019	45.214	242024.499	2.395
MF2(30)	0.604	32.781	1.095	28.192	0.630	6.050	0.013	32.830	244984.576	1.874

Table 6
Structural mortar and composite mortars flexural test properties.

	Deflection max. (d)		Strain energy		Flexural stress (σ)		Flexural strain (ε)		Moment of inertia (I)	
	Mean	Co.V	Mean	Co.V	Mean	Co.V	Mean	Co.V	Mean	Co.V
	mm	%	kNmm	%	MPa	%		%	mm^4	%
MS (no-fiber)	0.578	23.219	0.447	13.904	7.789	8.446	0.012	23.378	218301.931	1.872
MSF0.5(5)	0.381	22.855	0.677	28.459	5.045	13.572	0.008	23.405	243885.014	2.728
MSF0.5(10)	0.395	16.949	0.580	24.888	5.825	8.929	0.008	16.951	234638.973	1.794
MSF0.5(30)	0.402	20.196	0.903	18.180	6.287	3.701	0.008	21.916	235917.934	5.057
MSF1(5)	0.486	53.980	0.769	13.796	3.914	6.393	0.010	54.246	239304.314	3.153
MSF1(10)	0.350	5.229	0.959	25.123	4.131	16.062	0.007	5.540	233765.911	1.843
MSF1(30)	0.477	10.067	0.551	67.009	5.068	7.931	0.010	10.186	238971.074	2.457
MSF1.5(5)	0.372	17.944	0.688	13.872	3.062	9.176	0.008	18.528	230956.559	2.092
MSF1.5(10)	0.668	57.634	1.209	28.018	3.733	10.518	0.014	57.603	233274.868	0.618
MSF1.5(30)	0.461	24.379	1.470	41.546	4.455	8.069	0.010	24.534	236707.824	2.199
MSF2(5)	0.286	12.177	0.668	12.258	2.389	8.438	0.006	12.917	233151.347	2.644
MS F2(10)	0.331	19.738	1.180	16.676	2.719	6.838	0.007	20.645	236396.515	3.685
MSF2(30)	0.530	45.370	2.687	34.841	3.611	10.919	0.011	46.069	230882.531	3.098

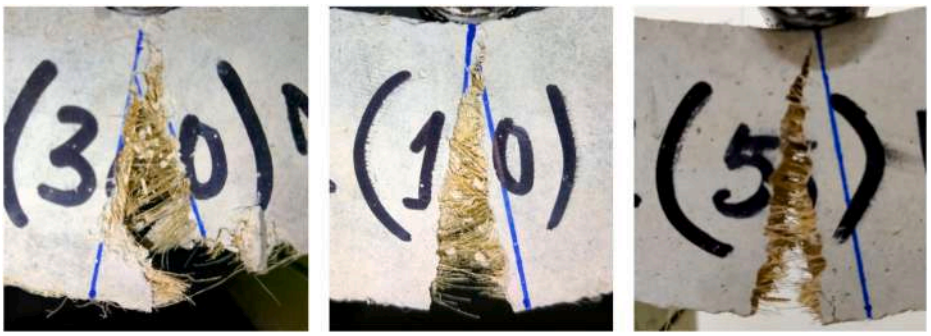

Fig. 15. Zoomed view of samples with (a) 30 mm, (b) 10 mm and (c) 5 mm long jute fibers with equal percentage (i.e 2% with respect to the day mortar mass).

In the case of samples with fibers (Fig. 14b), it has been noticed that even after reaching the maximum flexural strength the samples keep a residual softening behavior. Indeed, the presence of fibers improved the maximum deflection of the specimens, but also their strain energy capacity. It has been found that the flexural strength and strain energy decrease with the decrease of the fiber length Table 5 and Table 6. Longer fibers (Fig. 15) present a better mechanical performance in comparison to shorter ones.

Fig. 16, Fig. 17, Figs. 18 and 19 represent the experimental stress-strain curves comparison between the composite thermal mortar samples (with fibers) and the normal thermal mortar samples without fibers.

Looking at Fig. 16 it can be seen that samples with 0.5% fiber (with respect to the dry mortar mass) present a flexural strength reduction of 12.84% when fibers are 30 mm long, 33.62% when fibers are 10 mm long and 37.43% when fibers are 5 mm long.

Similarly, in Fig. 17, samples with 1% fiber (with respect to the dry mortar mass) present a strength drop of 54.29% when fibers are 30 mm long, 53.79% when fibers are 10 mm long and 68.17% when fibers are 5 mm long.

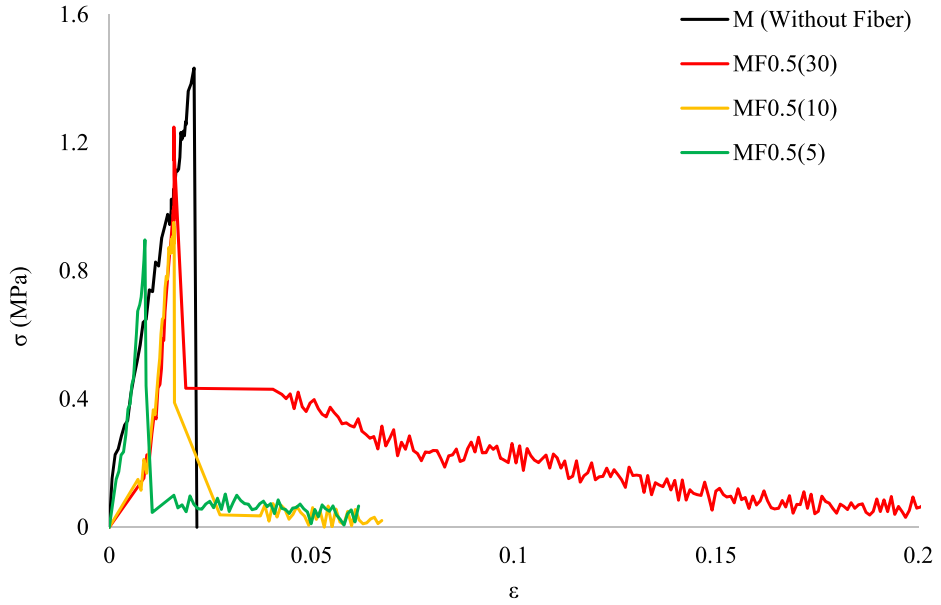

Fig. 16. Thermal mortar stress-strain curves: mortar sample Vs composite mortars samples with fiber lengths 30 mm, 10 mm and 5 mm with 0.5% fiber with respect to the dry mortar mass.

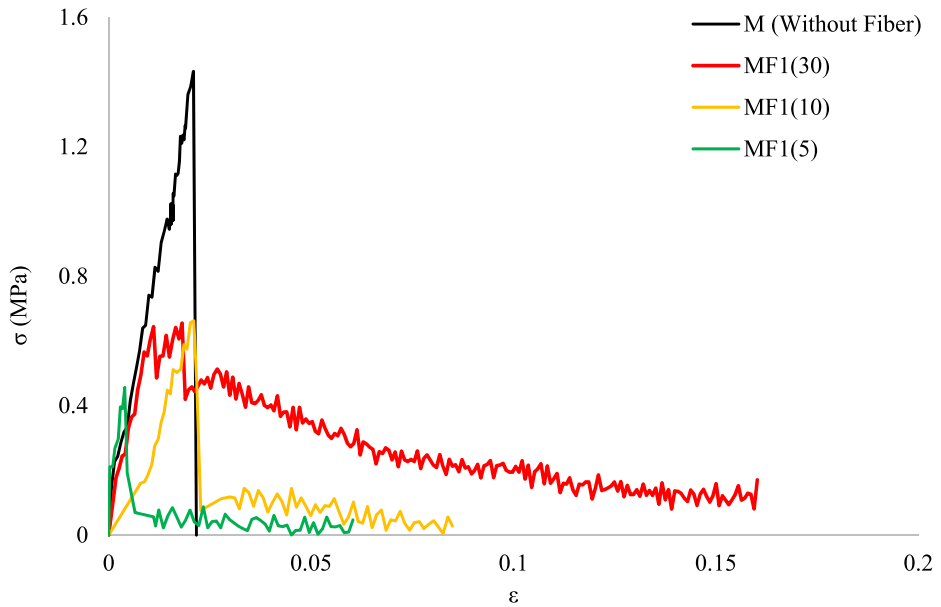

Fig. 17. Thermal mortar stress-strain curves: mortar sample Vs composite mortars samples with fiber lengths 30 mm, 10 mm and 5 mm with 1% fiber with respect to the dry mortar mass.

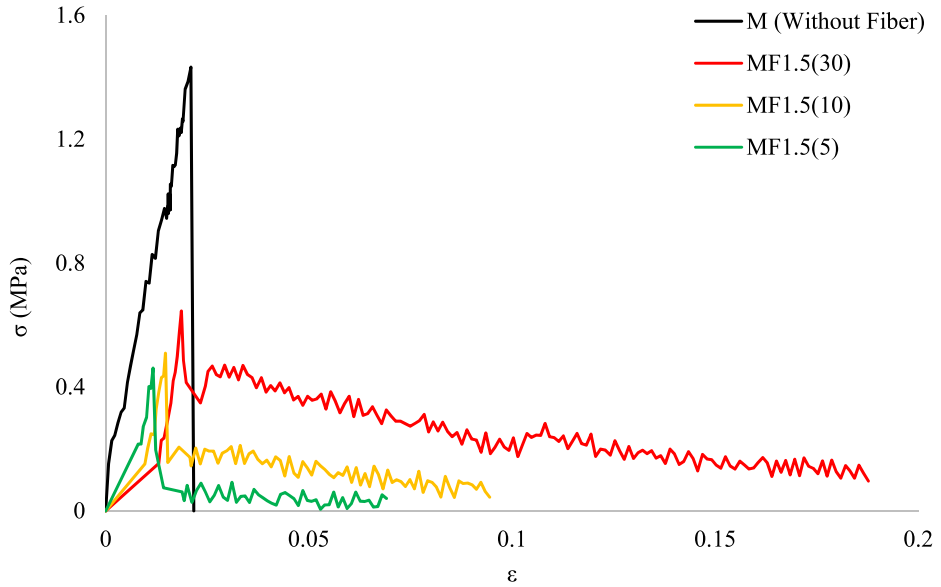

Fig. 18. Thermal mortar stress-strain curves: mortar sample Vs composite mortars samples with fiber lengths 30 mm, 10 mm and 5 mm with 1.5% fiber with respect to the dry mortar mass.

Fig. 18 shows that samples with 1.5% fiber (with respect to the dry mortar mass) have strength drop around 54.96% when fibers are 30 mm long, 64.47% when fibers are 10 mm long and 67.82% when fibers are 5 mm long.

Finally, Fig. 19 highlights that samples with 2% fiber (with respect to the dry mortar mass) present a strength reduction of 57.49% when fibers are 30 mm long, 76.29% when fibers are 10 mm long and 81.44% when fibers are 5 mm long.

Fig. 20, Fig. 21, Figs. 22 and 23 depict the stress-strain curves comparison of composite structural mortar samples (with fibers) and normal structural mortar samples without fibers.

Fig. 20 shows that samples with 0.5% fiber (with respect to the dry mortar mass) have a flexural strength reduction of 24.81% when fibers are 30 mm long, 30.59% when fibers are 10 mm long, and 36.77% when fibers are 5 mm long.

Similarly, Fig. 21 presents the results of samples with 1% fiber (with respect to the dry mortar mass) where there is a flexural

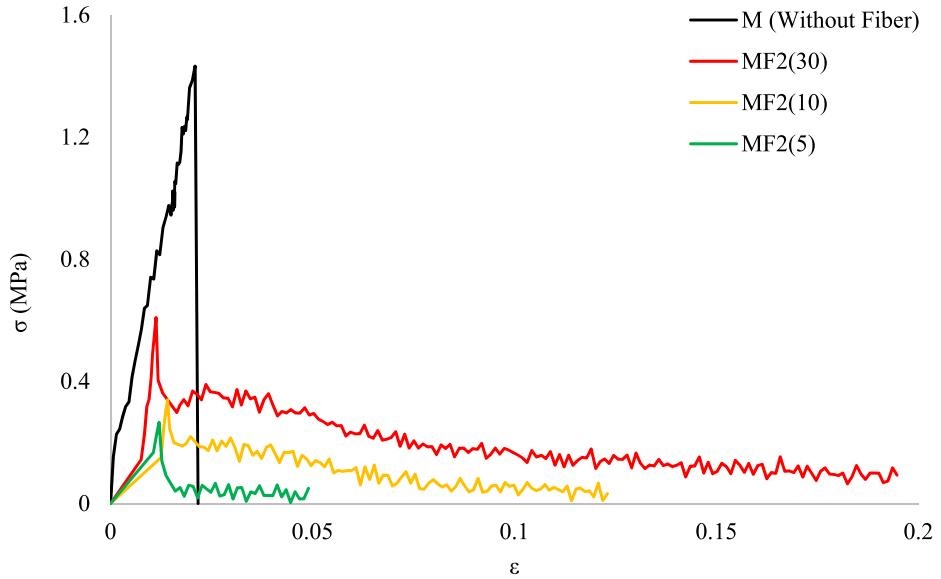

Fig. 19. Thermal mortar stress-strain curves: normal mortar sample Vs composite mortars samples with fiber lengths 30 mm, 10 mm and 5 mm with 2% fiber with respect to the dry mortar mass.

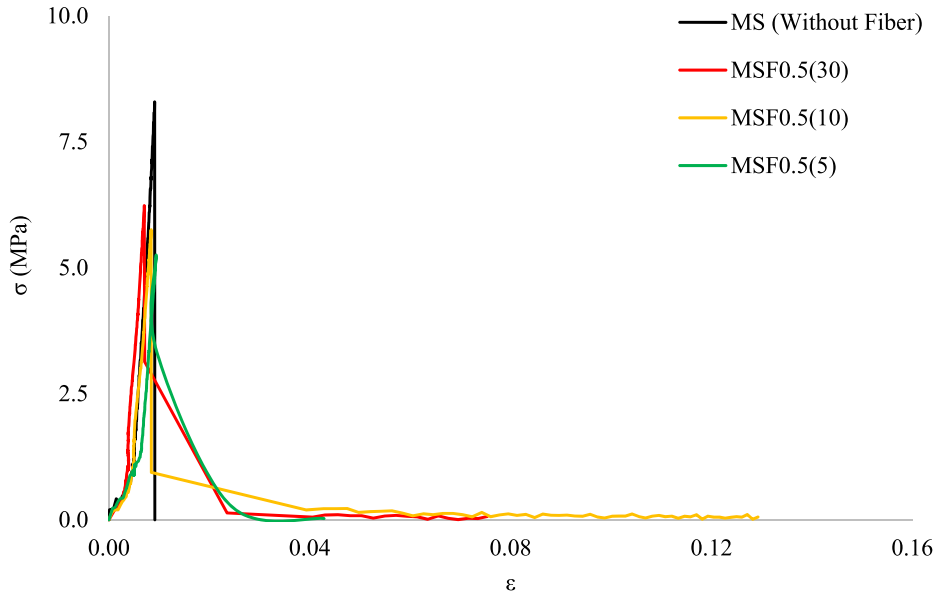

Fig. 20. Structural mortar stress-strain curves: mortar sample Vs composite mortars samples with fiber lengths 30 mm, 10 mm and 5 mm with 0.5% fiber with respect to the dry mortar mass.

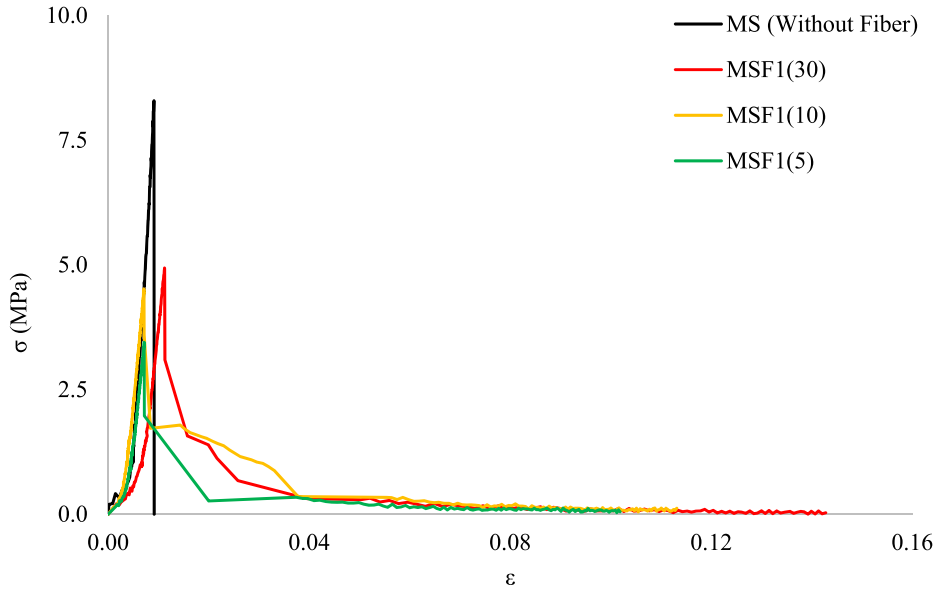

Fig. 21. Structural mortar stress-strain curves: mortar sample Vs composite mortars samples with fiber lengths 30 mm, 10 mm and 5 mm with 1% fiber with respect to the dry mortar mass.

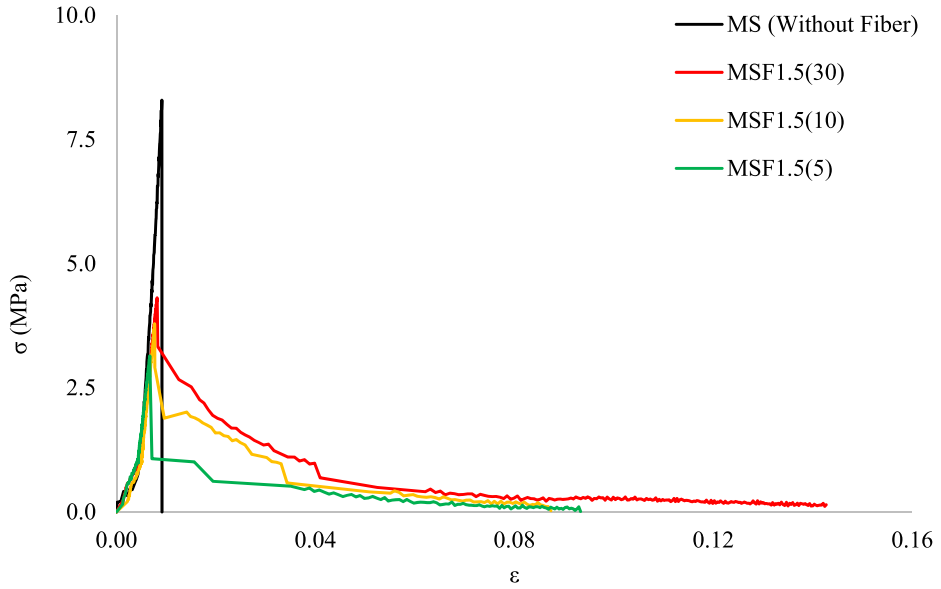

Fig. 22. Structural mortar stress-strain curves: mortar sample Vs composite mortars samples with fiber lengths 30 mm, 10 mm and 5 mm with 1.5% fiber with respect to the dry mortar mass.

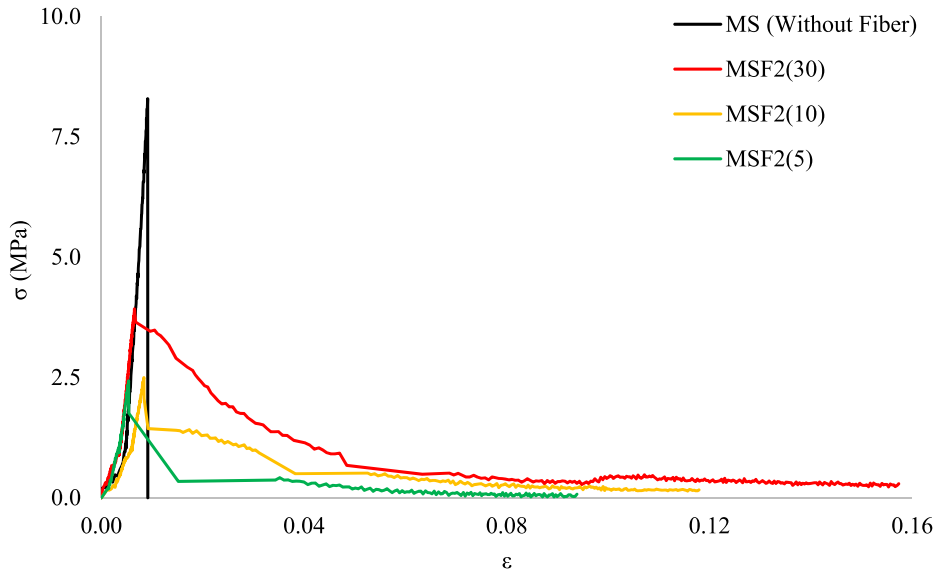

Fig. 23. Structural mortar stress-strain curves: mortar sample Vs composite mortars samples with fiber lengths 30 mm, 10 mm and 5 mm with 2% fiber with respect to the dry mortar mass.

strength drop of 40.45% when fibers are 30 mm long, 45.49% when fibers are 10 mm long, and 58.41% when fibers are 5 mm long.

The results for specimens with 1.5% fiber (with respect to the dry mortar mass) are presented in Fig. 22.

The following flexural strength reductions have been recorded: 47.99% when fibers are 30 mm long, 54.30% when fibers are 10 mm long and 62.09% when fibers are 5 mm long.

Lastly, in Fig. 23 it is possible to see the results for the specimens with 2% fiber (with respect to the dry mortar mass) where the following flexural strength reductions have been measured: 52.67% when fibers are 30 mm long, 69.89% when fibers are 10 mm long and 70.71% when fibers are 5 mm long.

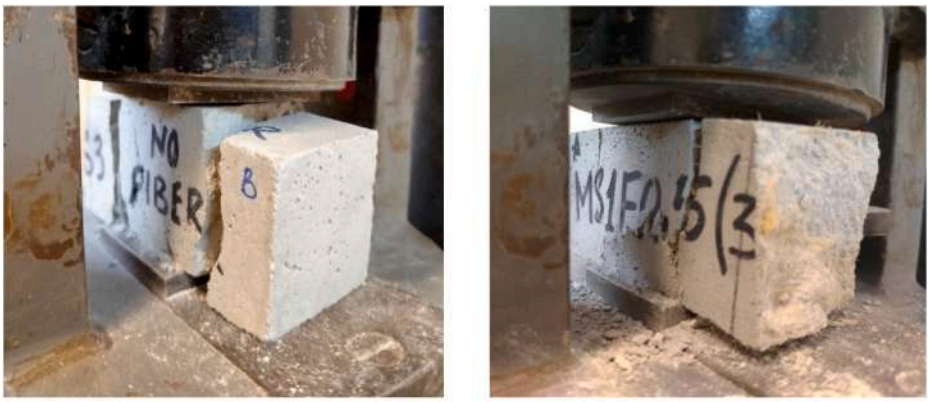

Fig. 24. Structural mortar samples ultimate compression rupture (a) MS3M1S3 without fiber and (b) MS1F0.5(30)M2S3 with 0.5% jute fiber (30 mm) with respect to the dry mortar mass.

3.2.2. Compression test

The compression tests were performed following the EN 1015-11 [69]. Fig. 24 represents the collapse conditions of samples without (Fig. 24 (a)) and with fibers (Fig. 24 (b)).

A typical hourglass collapse at compression failure has been observed for all structural and thermal mortar samples without fibers (Fig. 25).

After reaching the ultimate compressive load, composite mortar samples did not present any physical separations between the different damaged sample parts (Fig. 26 a and b). In the enlarged picture (Fig. 26c) it is possible to see that the embodied fibers help to hold the broken pieces together.

It has been observed that, as the fiber percentage and fiber length increases, the compressive strength decreases in comparison to the sample without fiber. This is true for both thermal and structural composite-mortars, see Table 7.

In the case of thermal composite-mortars the reduction in the compressive strengths, in samples with 0.5% fiber is 29.05% (5 mm fibers length), 32.85% (10 mm fibers length) and 9.81% (30 mm fibers length). For samples with 1% fiber there is a compressive strength drop of 66.77% (5 mm fibers length), 60.51% (10 mm fibers length) and 54.58% (30 mm fibers length). Samples with 1.5% fiber present a compressive strength drop of 78.65% (5 mm fibers length), 81.11% (10 mm fibers length) and 63.34% (30 mm fibers length). Finally, samples with 2.0% fibers show a compressive strength drop of 89.85% (5 mm fibers length), 83.70% (10 mm fibers length) and 41.37% (30 mm fibers length).

Similarly, in the case of structural composite mortars the reduction in the compressive strengths are respectively: for 0.5% fiber 24.84% (5 mm fibers length), 17.06% (10 mm fibers length) and 18.90% (30 mm fibers length); for 1.0% fiber 54.48% (5 mm fibers length), 44.09% (10 mm fibers length) and 32.33% (30 mm fibers length); for 1.5% fiber 66.56% (5 mm fibers length), 56.69% (10 mm fibers length) and 44.84% (30 mm fibers length); for 2.0% fiber 81.30% (5 mm fibers length), 73.96% (10 mm fibers length) and 68.53% (30 mm fibers length).

Fig. 25. Thermal mortar sample M1M2S2 without fiber, after compression failure.

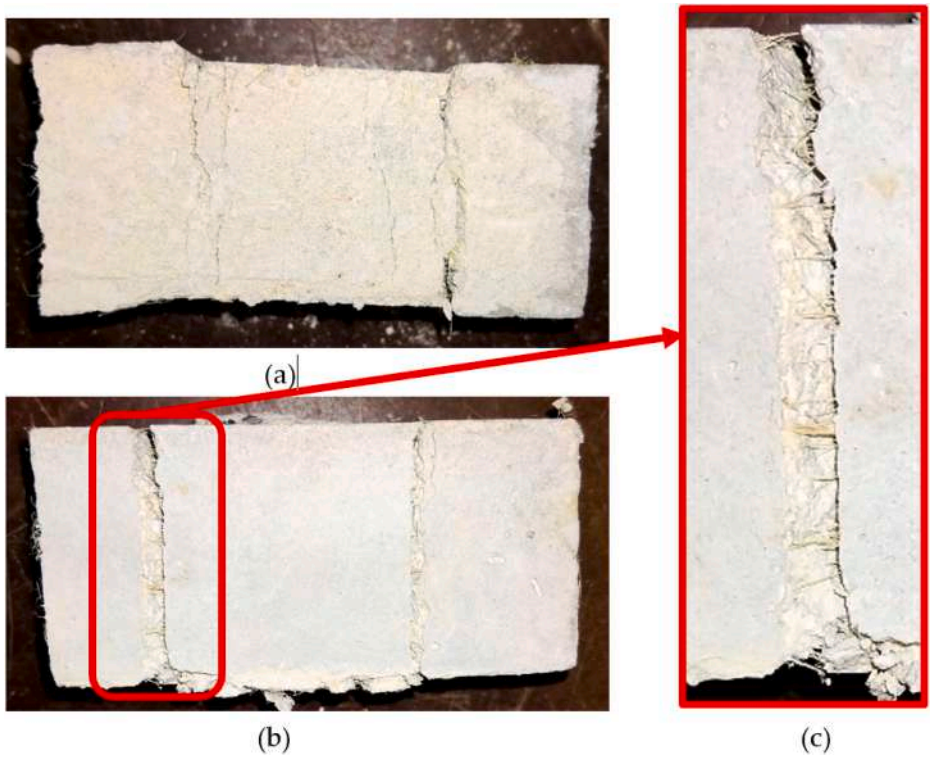

Fig. 26. Structural mortar sample MS1F0.5(30)M1S2 (a) bottom view, (b) back view and (c) enlarged view, retrofitted with 0.5% jute fiber (30 mm) with respect to the dry mortar mass.

Table 7
Compressive strength (Rc).

Thermal mortar and composite mortars			Structural mortar and composite mortars		
	Mean	Co.V		Mean	Co.V
	MPa	%		MPa	%
M (No fiber)	3.50	9.69	MS (No fiber)	32.25	5.61
MF0.5(5)	2.48	7.79	MSF0.5(5)	24.24	4.84
MF0.5(10)	2.35	6.62	MSF0.5(10)	26.75	2.12
MF0.5(30)	3.15	2.33	MSF0.5(30)	26.16	6.89
MF1(5)	1.16	12.56	MSF1(5)	14.68	15.82
MF1(10)	1.38	3.62	MSF1(10)	18.03	10.41
MF1(30)	1.59	3.49	MSF1(30)	21.83	5.79
MF1.5(5)	0.75	10.03	MSF1.5(5)	10.79	4.72
MF1.5(10)	0.66	16.27	MSF1.5(10)	13.97	3.02
MF1.5(30)	1.28	6.16	MSF1.5(30)	17.79	3.97
MF2(5)	0.36	34.77	MSF2(5)	6.03	7.47
MF2(10)	0.57	9.37	MSF2(10)	8.40	12.35
MF2(30)	2.05	9.19	MSF2(30)	10.15	7.41

Figs. 27 and 28 show the linear trends of reducing the compressive strengths with respect to the combination of increase in fiber percentages and variation in fiber lengths (see Table 8).

3.3. Thermal properties and observations

The unreinforced thermal and structural mortars (without fibers), and jute fiber thermal and structural composite mortars insulating performances have been evaluated by comparing their thermal conductivities. Fig. 29 presents the Thermal Conductivity (TC) of structural and thermal mortars versus different temperatures. The presence of approximatively spherical recycled aggregates (section 2.3.1.1, Fig. 7) provides lower TC values to thermal mortar. After oven drying, the normal thermal mortar has the following TC values: 0.230 W/mK at10 °C), 0.236 W/mK (at 20 °C) and 0.241 W/mK (at 30 °C), whereas the normal structural mortar has the TC values equal to 0.759, 0.771 and 0.793 W/mK respectively (at 10, 20 and 30 °C). Linear trends of the TC have been observed for all samples, with minimum and maximum values corresponding to 10 °C and 30 °C, respectively, see Table 9 for regression data. Actually, this is a first estimation of the trends and of the deviations that would require a higher number of observations to be accurate. Figs. 30 and 31

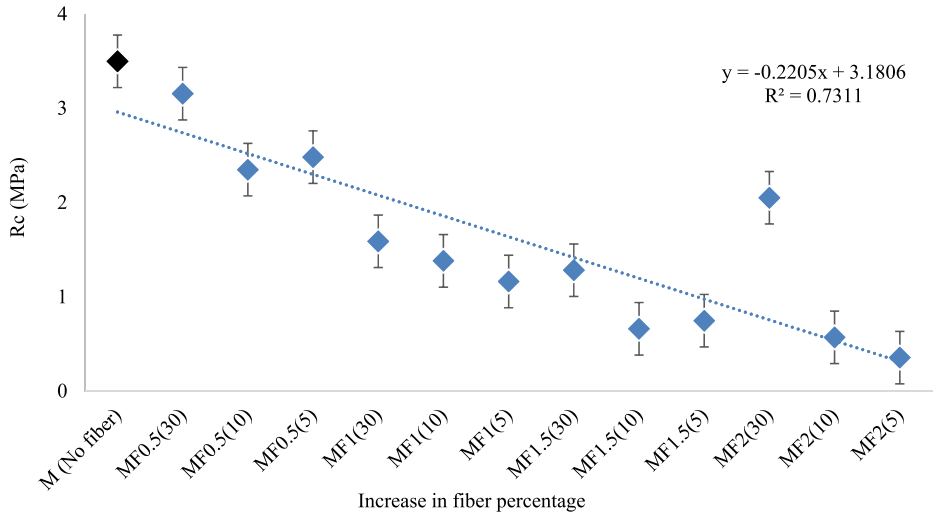

Fig. 27. Compression strengths of the thermal mortar and composite mortars with different fiber lengths (30 mm, 10 mm and 5 mm) and various fiber percentages (0.5%, 1%, 1.5% and 2% w.r.t mortar mass).

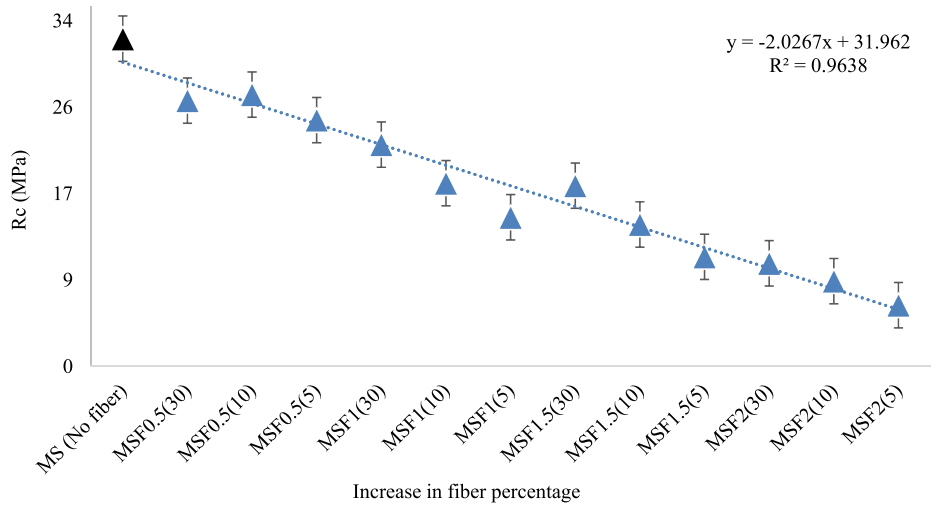

Fig. 28. Compression strengths of the structural mortar and composite mortars with different fiber lengths (30 mm, 10 mm and 5 mm) and various fiber percentages (0.5%, 1%, 1.5% and 2% w.r.t mortar mass).

Table 8
Linear Regression respect to the compression strength graphs.

	A	B	R^2
Thermal mortar (Fig. 27)	−0.2205	3.1806	0.7311
Structural mortar (Fig. 28)	−2.0267	31.962	0.9638

represent the TC values of the thermal and structural composite mortars, respectively. In these figures only the TC values of the samples after moisture removal through oven drying (for details see Section 2.3.3) have been represented. It is evident that in both cases, with the increase in fiber percentages (with respect to the mortar mass) the TC value decreases, therefore the insulating capacity of the composite mortars improve linearly. Moreover, in the same fiber percentage category (i.e., 0.5%, 1%, 1.5% and 2% with respect to the mortar mass), it has been observed that the small fibers have better performances than longer ones.

Comparing the measured TC values (at 10 °C, 20 °C and 30 °C) of the normal thermal mortar M-(No fiber) with the TC values of the samples with fibers we can underline that the TC measurements are always decreasing when the fiber percentage and the mean temperature are increased, see Fig. 30, Table 10 and Table 11. The decreasing percentage varies in average between 0.1% and 3% with a peak decreasing value equal to 6.5% recorded for the sample MF2(5) from 20 °C to 30 °C. These reductions in TC, highlight the

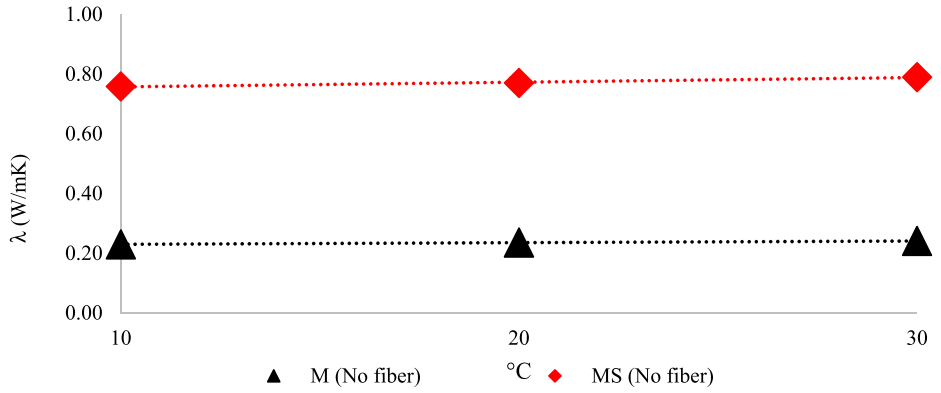

Fig. 29. Thermal conductivity comparison: thermal mortar Vs. structural mortar, without fiber.

Table 9
Linear Regression respect to the thermal conductivity trends.

Thermal mortar –> M (No fiber)	0.0006	0.2241	0.9958
Structural mortar – >MS (No fiber)	0.0016	0.7414	0.9745

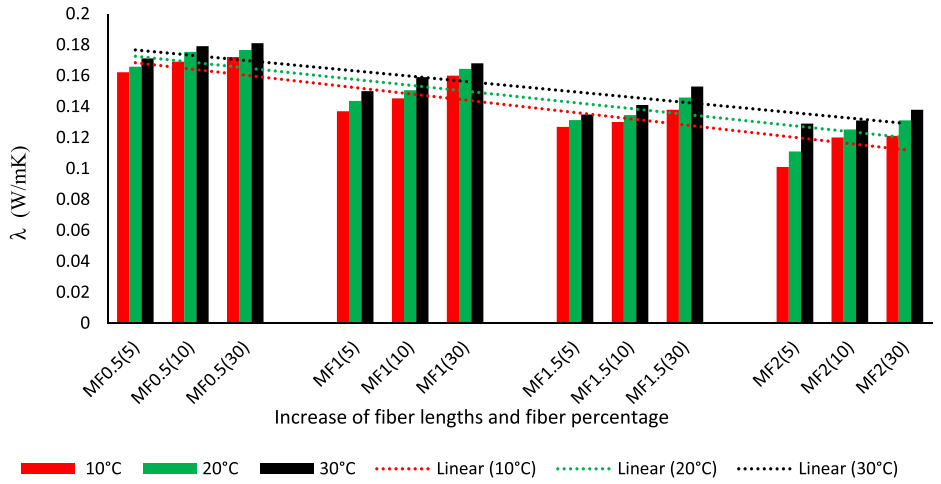

Fig. 30. TC after oven drying: Reduction in TC values of the thermal composite mortars with the increase of fiber percentages.

Table 10
Linear regression respect to the thermal conductivity trends with fiber percentage increment.

	A	B	R^2
Fiber percentage increment at 10 °C	−0.004	0.1724	0.7500
Fiber percentage increment at 20 °C	−0.0038	0.1763	0.7302
Fiber percentage increment at 30 °C	−0.0034	0.1800	0.7461

improvement of the insulating capacity of each composite mix.

While comparing the measured TC values (at 10 °C, 20 °C and 30 °C) of the normal structural mortar MS (No fiber) with the TC values of the thermal-composite mortar samples (fibers used with respect to mortar mass) we can underline that the TC values almost always decrease with increasing mean temperature and fiber percentage (see Fig. 31, Table 12, Table 13). Here, the decreasing percentage varies in average between 0.1% and 3% with a peak decreasing value equal to 11.4% recorded for the sample MSF1.5(10) from 10 °C to 20 °C. These reductions in TC, highlight the improvement of the insulating capacity of each individual composite mix.

In general, the reduction of density leads to a reduction of thermal conductivity and vice versa. Thus, the addition of fibers to the mortar mixes produces an increase of the porosity and a reduction of density, consequently it leads also to a reduction of the thermal conductivity. At the same time the reduction of density produces a reduction of the compressive strength and elastic modulus of the

Table 11
The percentage reduction in thermal conductivity value [λ (W/mK)] of the thermal composite mortars, when compared with the sample without fiber i.e. M (No fiber).

	λ (W/mK)		
	10 °C	20 °C	30 °C
M (no fiber) Reference value	0,230	0,236	0,241
MF0.5(5)	−29.32%	−29.66%	−28.86%
MF0.5(10)	−26.36%	−25.58%	−25.62%
MF0.5(30)	−25.05%	−25.08%	−24.79%
MF1(5)	−40.31%	−39.03%	−37.67%
MF1(10)	−36.69%	−36.11%	−33.93%
MF1(30)	−30.28%	−30.25%	−30.19%
MF1.5(5)	−44.71%	−44.29%	−43.94%
MF1.5(10)	−43.36%	−42.89%	−41.41%
MF1.5(30)	−39.87%	−38.10%	−36.42%
MF2(5)	−55.99%	−52.91%	−46.40%
MF2(10)	−47.71%	−46.88%	−45.56%
MF2(30)	−47.23%	−44.38%	−42.66%

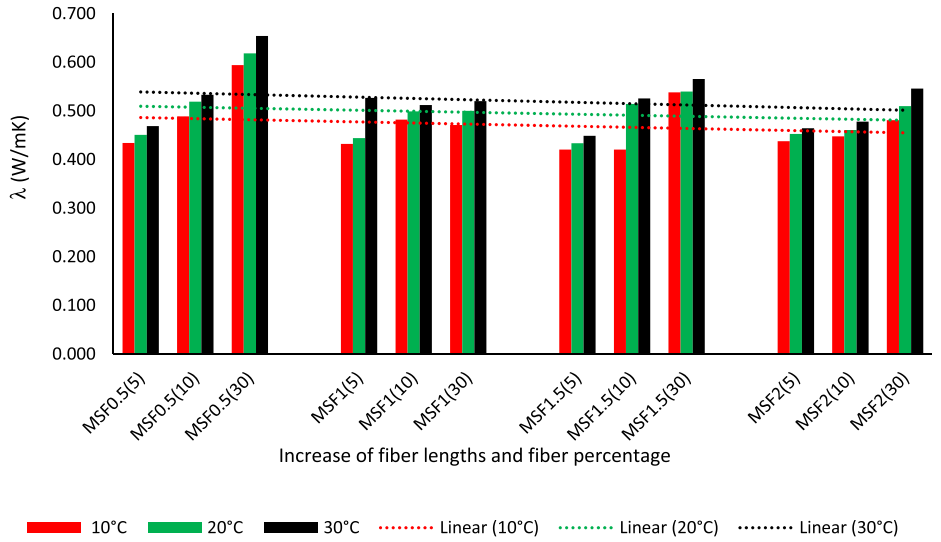

Fig. 31. *TC after oven drying:* Reduction *in TC values* of the structural composite mortars with the increase of fiber percentages.

Table 12
Linear regression respect to the thermal conductivity trends with fiber percentage increment.

	A	B	R^2
Fiber percentage increment @ 10 °C	−0.0022	0.4885	0.0417
Fiber percentage increment @ 20 °C	−0.0021	0.5116	0.0353
Fiber percentage increment @ 30 °C	−0.0027	0.5417	0.0533

composite material. However, as can be noticed in Figs. 30 and 31, the effect induced by an increase (in %) in the amount of fibers risks being nullified by their length. It is possible to notice how the increase of their linear dimension, with the same % by weight in the material, leads to a worsening of the thermal properties. This is presumably caused by an increase in the preferential paths of the heat in crossing the material, facilitated by the presence of longer and intertwined fibers which guarantee greater continuity to the flow, compared to shorter and better distributed fibers in the product.

The results presented in Section 3.2 and 3.3 confirm these observations underlining these opposite trends in material characteristics after the fiber addition: on one side it improves the thermal behavior on the other side it reduces the mechanical performance. Section 3.4 will discuss the integrated behavior of composite mortars taking into account other aspects of the mechanical properties.

Table 13
The percentage-reduction in thermal conductivity value [λ (W/mK)] of the structural composite mortars, when compared with the sample without fiber i.e. MS (No fiber).

	λ (W/mK)		
	10 °C	20 °C	30 °C
MS (no fiber) Reference value	0,759	0,771	0,793
MSF0.5(5)	−42.75%	−41.46%	−40.67%
MSF0.5(10)	−35.57%	−32.57%	−32.51%
MSF0.5(30)	−21.67%	−19.70%	−17.17%
MSF1(5)	−43.05%	−42.32%	−33.29%
MSF1(10)	−36.45%	−35.17%	−35.17%
MSF1(30)	−37.90%	−35.04%	−34.16%
MSF1.5(5)	−44.57%	−43.69%	−43.16%
MSF1.5(10)	−44.57%	−33.19%	−33.46%
MSF1.5(30)	−29.06%	−29.90%	−28.39%
MSF2(5)	−42.29%	−41.19%	−41.21%
MSF2(10)	−40.96%	−40.14%	−39.50%
MSF2(30)	−36.59%	−33.74%	−30.87%

3.3.1. *The influence of moisture on thermal conductivity*

In order to evaluate the influence of moisture on TC value a total of five (see Table 14) measurements have been carried out on each sample on 10th, 15th, 22nd and 28th day of the natural drying period. Whereas the final measurement has been conducted, after forced oven drying. Fig. 32, Figs. 33 and 34 represent the change and decrease in TC with the reduction of moisture in the samples MSF1(30), MS1(10) and MSF1(5) respectively, see Table 15 for regression data. The reduction in TC indicates the improvement of samples insulating capacity. From the first TC measurement conducted on the 10th day of natural drying to the forced oven drying TC measurement approximately 37.9%, 36.6% and 28.6% reduction in TC and 10.4%, 11.2% and 10.9% reduction in sample masses have been observed for the samples MSF1(30) (Fig. 32), MS1(10) (Fig. 33) and MSF1(5) (Fig. 34), respectively. It is possible to note that, in average, water presence influences the TC measurement producing 1% TC reduction for 1 g of mass reduction during natural drying. At the end of this period the sample has brought itself to thermodynamic equilibrium with the test environment (the humidity of the laboratory is kept at 60% + - 10%). Complete drying is achieved (for the samples MSF1(30) on 43rd day, MS1(10) on 40th day and MSF1(5) on 44th day) by keeping the sample in the oven at a constant temperature of 50 °C for about 10 days, at the end of which the last weight and thermal conductivity measurement was performed.

Table 14
Thermal conductivities of the structural mortars.

Drying days	λ (W/mK)											
	10 °C	20 °C	30 °C	10 °C	20 °C	30 °C	10 °C	20 °C	30 °C	10 °C	20 °C	30 °C
	0.5% of fiber with respect to mortar mass			1% of fiber with respect to mortar mass			1.5% of fiber with respect to mortar mass			2% of fiber with respect to mortar mass		
	MSF0.5(5)			MSF1(5)			MSF1.5(5)			MSF2(5)		
10th day of natural drying	0.547	0.566	0.598	0.598	0.621	0.650	0.637	0.692	0.757	0.685	0.735	0.741
15th day of natural drying	0.482	0.511	0.555	0.524	0.555	0.597	0.569	0.611	0.647	0.491	0.519	0.564
22nd day of natural drying	0.449	0.471	0.497	0.537	0.554	0.578	0.548	0.569	0.591	0.475	0.491	0.510
28th day of natural drying	0.451	0.462	0.475	0.533	0.551	0.573	0.448	0.466	0.489	0.468	0.482	0.504
After oven drying	0.434	0.451	0.469	0.432	0.444	0.527	0.420	0.433	0.449	0.438	0.453	0.464
	MSF0.5(10)			**MSF1(10)**			**MSF1.5(10)**			**MSF2(10)**		
10th day of natural drying	0.707	0.742	0.797	0.744	0.787	0.832	0.696	0.749	0.817	0.800	0.866	0.940
15th day of natural drying	0.522	0.553	0.576	0.608	0.659	0.679	0.589	0.624	0.674	0.502	0.547	0.603
22nd day of natural drying	0.527	0.544	0.566	0.540	0.561	0.577	0.520	0.534	0.553	0.460	0.477	0.501
28th day of natural drying	0.521	0.532	0.549	0.524	0.542	0.573	0.503	0.520	0.543	0.437	0.452	0.469
After oven drying	0.489	0.519	0.533	0.482	0.499	0.512	0.420	0.514	0.526	0.448	0.461	0.478
	MSF0.5(30)			**MSF1(30)**			**MSF1.5(30)**			**MSF2(30)**		
10th day of natural drying	0.833	0.906	0.974	0.672	0.805	0.851	0.746	0.800	0.866	0.658	0.672	0.707
15th day of natural drying	0.781	0.840	0.898	0.567	0.721	0.736	0.569	0.629	0.664	0.558	0.636	0.651
22nd day of natural drying	0.707	0.729	0.756	0.485	0.563	0.583	0.547	0.579	0.599	0.569	0.589	0.617
28th day of natural drying	0.616	0.635	0.680	0.536	0.557	0.583	0.554	0.572	0.592	0.497	0.519	0.574
After oven drying	0.594	0.618	0.654	0.471	0.500	0.520	0.538	0.540	0.566	0.481	0.510	0.546

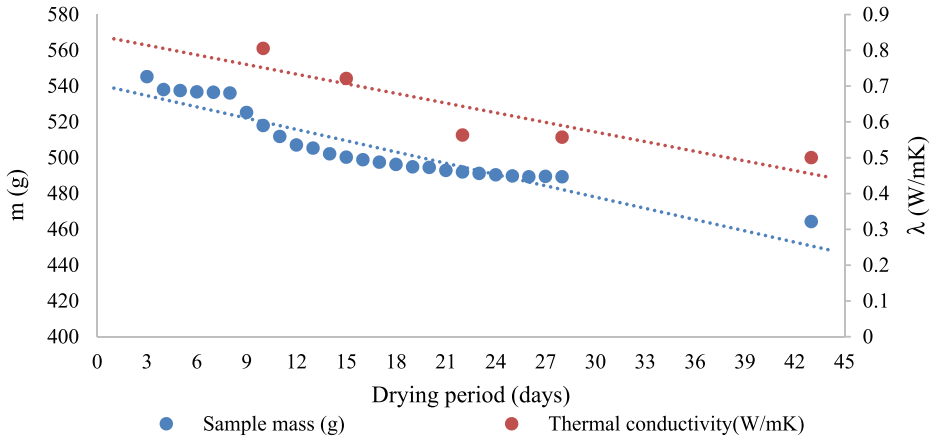

Fig. 32. MS1F1(30)T1 - Change in thermal conductivity with respect to the change in sample mass.

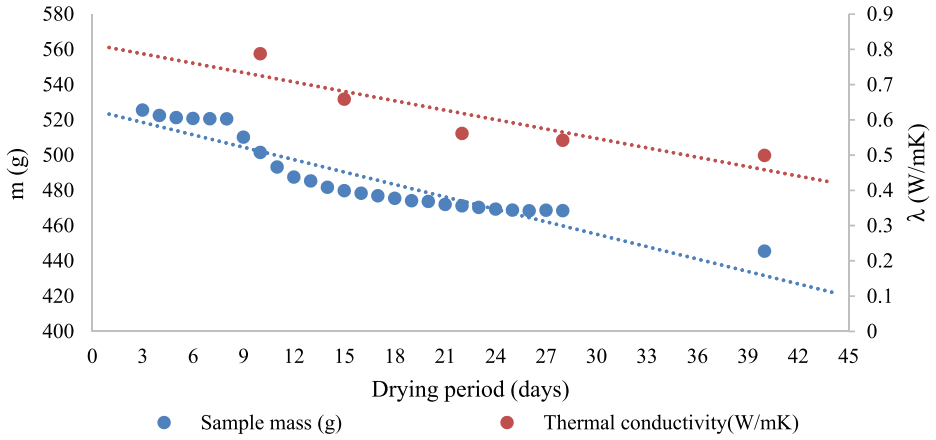

Fig. 33. MS1(10)T1 - Change in thermal conductivity with respect to the change in sample mass.

Table 15
Linear Regression respect to the mass and thermal conductivity trends with respect to the drying period.

		A	B	R^2
MS1F1(30)T1 (Fig. 32)	Mass (g)	−2.0983	540.96	0.8717
	Thermal conductivity (W/mK)	−0.0090	0.8410	0.8068
MS1F1(10)T1 (Fig. 33)	Mass (g)	−2.3496	525.61	0.8680
	Thermal conductivity (W/mK)	−0.0089	0.8140	0.8150
MS1F1(5)T1 (Fig. 32)	Mass (g)	−2.3260	521.38	0.8095
	Thermal conductivity (W/mK)	−0.0046	0.6536	0.8888

3.4. Integrated properties and observations

3.4.1. Flexural strength vs strain energy

The force (F) - displacement (δ) curves of some significative thermal mortar samples without fiber (Fig. 35a) and composite thermal mortar samples with 2% fiber (with respect to the mortar mass) and with 30 mm, 10 mm and 5 mm fiber lengths are shown in Fig. 35 b, Fig. 35c and Fig. 35 d, respectively. In the case of the thermal mortar, the strain energy capacity has been increased near about 442% and 8% for 30 mm (Fig. 35b) and 10 mm (Fig. 35c), respectively, while strain energy capacity reduced by 67% for 5 mm (Fig. 35c) fiber lengths. The comparison is proposed with reference to the sample M4M1S3 without fiber.

The force (F) - displacement (δ) curves of some significative structural mortar samples without fiber (Fig. 36a) and composite thermal mortar samples with 2% fiber (with respect to the mortar mass) and with 30 mm, 10 mm and 5 mm fiber lengths are shown in

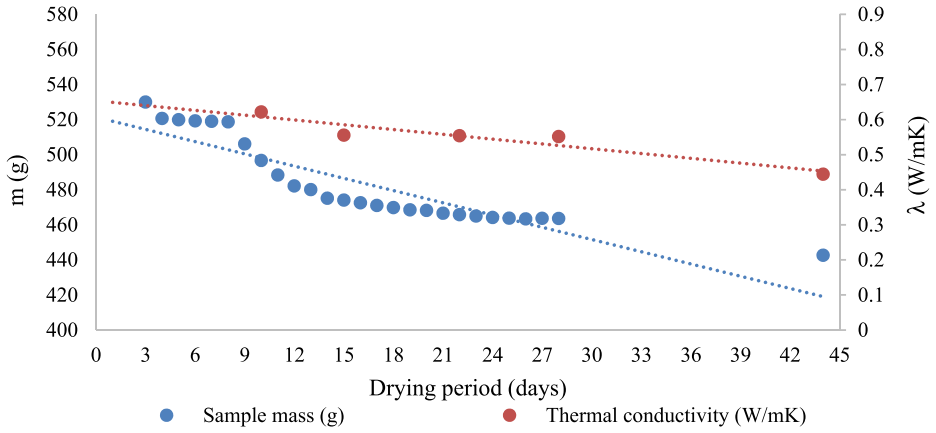

Fig. 34. MS1F1(5)T1 - Change in thermal conductivity with respect to the change in sample mass.

Fig. 36b,c and d, respectively.

Instead, in the case of the structural mortar, the strain energy capacity has been increased near about 547%, 217% and 98% for 30 mm (Fig. 36b) and 10 mm (Fig. 36c) and 5 mm (Fig. 36d) fiber lengths respectively. The comparison is done with reference to the sample MS1M2S2 without fiber.

Fig. 37 presents the deformed sample (with 1% fiber (30 mm) with respect to the dry mortar mass) at flexural ultimate limit state. It can be clearly seen how the fibers in the cross section lower part still transfer tensile loads even if the mortar matrix is already cracked.

Although due to the presence of the embodied fibers, the flexural strength of the composite-samples reduces, the strain energy capacity increases. This improved strain energy capacity is useful when it is necessary to dissipate the effects of extreme loads like earthquakes.

3.4.2. Compressive strength vs thermal conductivity

Figs. 38 and 39 represent the integrated (thermal and structural) behavior of the thermal and structural composite mortars. It is clearly visible that compression strengths reduce gradually with respect to the fiber percentages (from 0.5 to 1%, 1.5% and 2%) and fiber lengths (from 30 mm to 10 mm and 5 mm), so as the thermal conductivity values.

When composite mortars have been compared with non-reinforced mortars (without fiber), a drop in compressive strength and an improvement in insulating property (with the reduction of TC) have been observed (see Fig. 38 for thermal mortar samples and Fig. 39 for structural mortar samples). Table 16 and Table 17 represent the average percentage variation of the thermal and structural composite mortars compressive strength and TC with respect to the corresponding mortar sample without fiber.

3.5. Integrated analyses on alternative mixes

3.5.1. Case 1: composite mortar using SAW

The mechanical and thermal properties of the jute fiber (0.5% and 1% with respect to the thermal and structural mortar masses) composite mortars have been studied, by using Same Amount of Water SAW percentage with respect to the total mortar mixture mass (dry mortar + fiber), as in Table 18.

In this case the mixing time was 7–10 min. The mechanical properties of these composite samples are presented in Table 19, Table 20 and Table 21 and Figs. 40–43.

Considering the thermal mortar it has been observed that samples cast with SAW present strain energy capacities and flexural strengths (as in Fig. 40), and compressive strengths (Fig. 42) higher than those of samples casted in the previous phase (section 3.3.2) with different percentage of waters.

Actually, it has been found exactly to be opposite in the case of the structural composite mortars (Figs. 41 and 43). This can be explained considering the different properties of the two starting mortars: thermal and structural. The chosen SAW for the structural mortar is lower than the optimal one while in case of thermal mortar the obtained SAW mix is optimal from the mechanical properties point of view.

3.5.2. Case 2: thermal mortar without recycled aggregates (nRA) and SAW

In this case, recycled aggregates (RA), present in the commercial product, have been removed from the thermal mortar (Fig. 7b). Therefore, these insulation materials have been replaced with jute fibers. In this case the composite-mortars were prepared only using 30 mm, 10 mm and 5 mm fiber lengths and 1% fiber with respect to the dry mortar (without recycled aggregates - nRA) mass.

The samples with nRA have shown better mechanical performance in comparison to samples with-RA and without fiber (Sample M in Fig. 44), see Table 22, with increments in strain energy capacity and flexural stress of about 197.64% and 29.00% for 5 mm fiber length, 535.08% and 41.11% for 10 mm fiber length and 827.46% and 39.78% for 30 mm fiber length, respectively.

Similarly, the improvements for the nRA samples in the strain energy and the flexural stress of 2696.23% and 247.87% for 5 mm fiber length; 416.78% and 146.43% for 10 mm fiber length and 207.01% and 154.72% for 30 mm fiber length, were obtained with

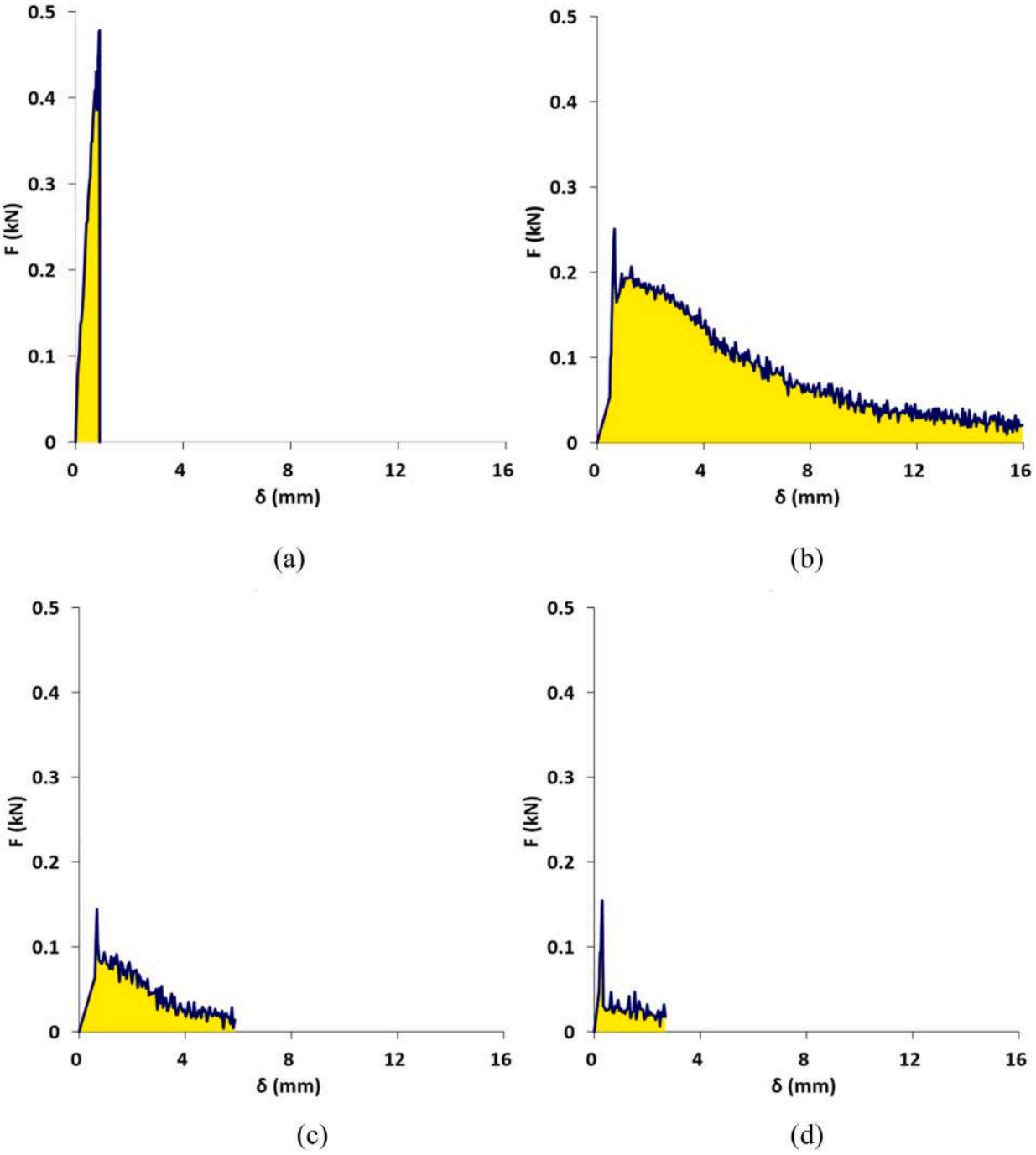

Fig. 35. Thermal mortars and composite-mortars strain energy graph (a) M4M1S3 (without fiber), (b) M1F2(30)M1S4, (c) M1F2(10)M1S3 and (d) M1F2(5)M2S2.

respect to the samples (MF1 in Fig. 44) with RA and 1% of fiber (with respect to mortar mass).

Likewise, Table 23 when the compression strength of the nRA samples were compared with the samples (M – No fiber Fig. 45) with RA and without fiber, an increment of 31.93% for 5 mm fiber length, 42.86% for 10 mm fiber length and 50.58% for 30 mm fiber length have been observed. Similarly, comparing with the samples (MF1 in Fig. 45) with RA and 1% fiber, an increment of 297.06% for 5 mm fiber length, 231.76% for 10 mm fiber length and 231.51% for 30 mm fiber length have been observed for the nRA samples. Whereas the improvement of 15.43% for 5 mm fiber length, 3.18% for 10 mm fiber length and 7.43% for 30 mm fiber length were obtained, when compared with samples (M(SAW)F1 in Fig. 45) with RA and SAW.

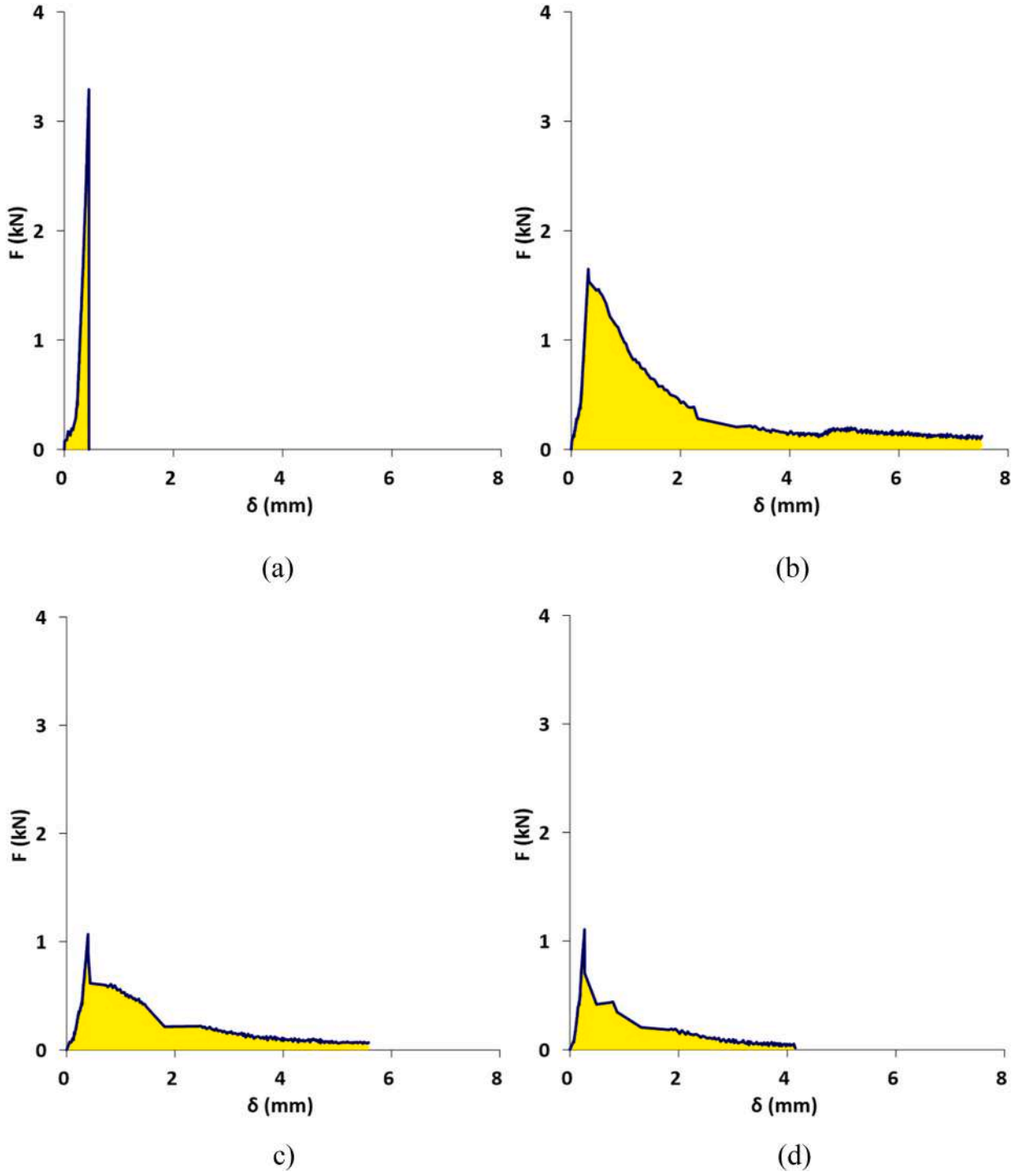

Fig. 36. Structural mortars and composite-mortars strain energy graph (a) MS1M2S2 (without fiber), (b) MS2F2(30)M2S2, (c) MS2F2(10)M2S2 and (d) MS2F2 (5)M1S2.

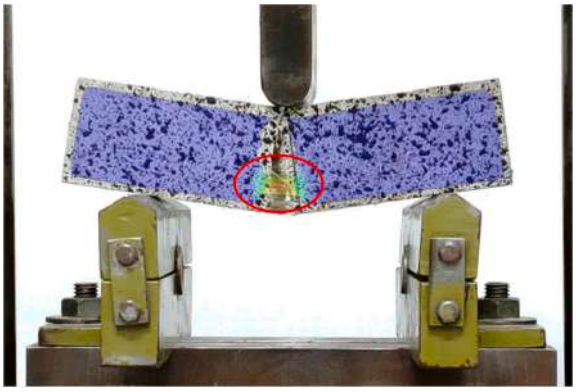

Fig. 37. MS1F1(30)M1S3(SAW) composite SM sample with 1% fiber (30 mm) with respect to the dry mortar mass.

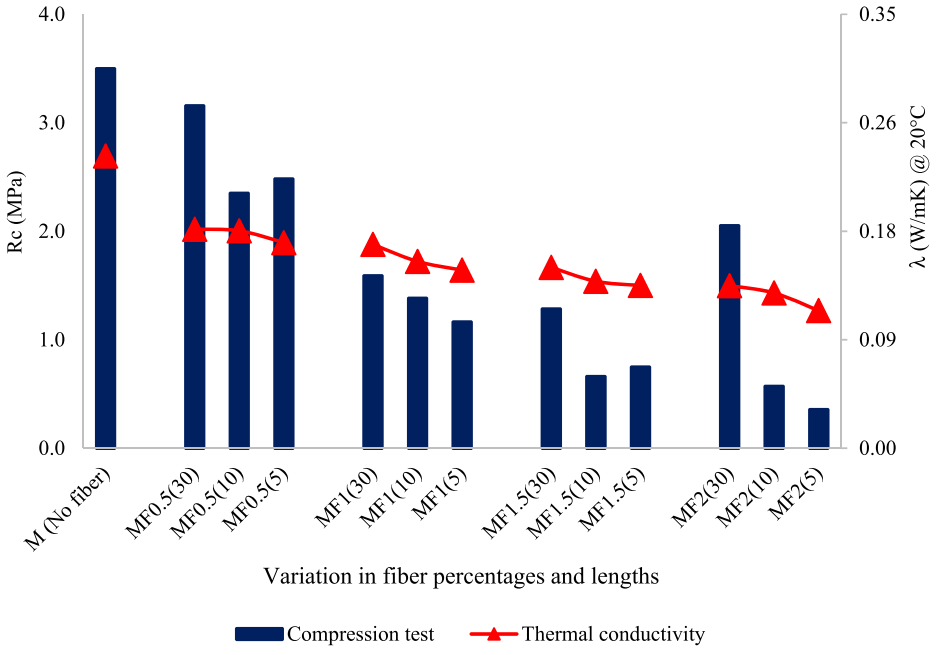

Fig. 38. Thermal mortars: compressive strength & thermal conductivity graph.

3.5.3. Case 3: Recycled Jute Fiber Composite Mortar (RJFCM)

This particular activity has been conducted keeping in mind the projects global and overall sustainability, therefore the residual jute fibers were collected during the net fabrication (class 1 mm threads) and the Recycled Jute Fiber Composite Mortar (RJFCM) were prepared.

A thermal mortar with the specification, as highlighted in Section 2.3.1.1 have been used for the preparation recycled jute thread fiber composite samples. Approximately 444.27 kg/m^3 of recycled aggregates can be present in a normal mortar sample, these recycled aggregates have been replaced with 77.5 kg/m^3 recycled jute thread fibers.

The mechanical behaviors were evaluated through flexural (Fig. 46a) and compressive (Fig. 46b) strengths. In this case, when we compare the mechanical results of the M – No fiber (with insulating ball) sample to these samples with recycled jute fibers it is possible to note a flexural strength clear reduction and a strain energy (Table 24), and compressive strength (Table 25) increase.

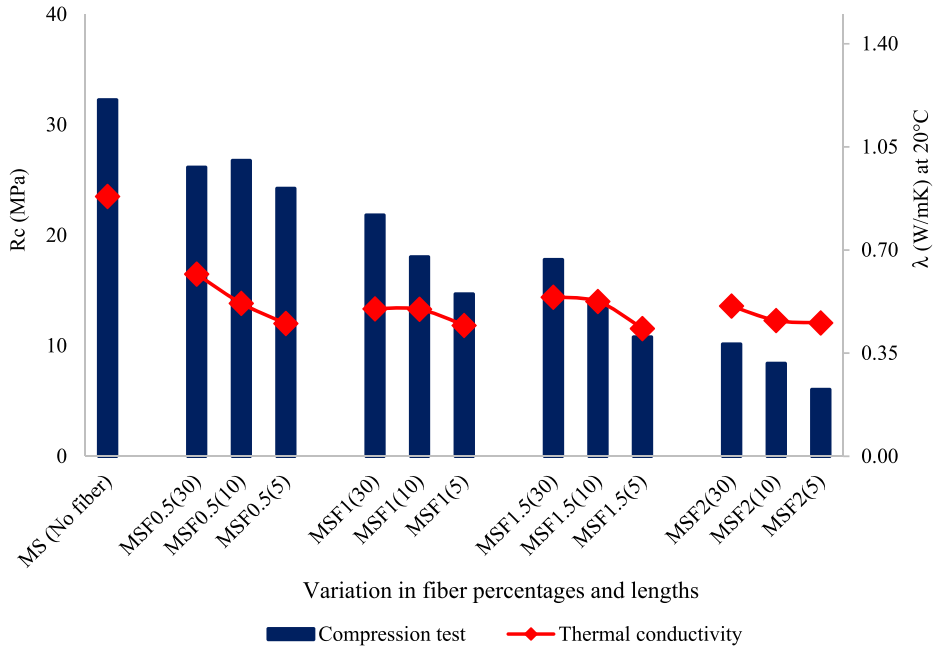

Fig. 39. Structural mortars: compressive strength & thermal conductivity graph.

Table 16
Integrated comparative behavior of the thermal composite mortars with respect to thermal mortar sample without fiber.

Fiber percentage with respect to the mortar mass	Reduction in compressive strength	Improvement in insulating capacity (with reduction in thermal conductivity at 20 °C)
0.5% (avg. of 5 mm, 10 mm and 30 mm)	−23.91%	26.77%
1.0% (avg. of 5 mm, 10 mm and 30 mm)	−60.62%	35.13%
1.5% (avg. of 5 mm, 10 mm and 30 mm)	−74.37%	41.76%
2.0% (avg. of 5 mm, 10 mm and 30 mm)	−71.64%	48.06%

Table 17
Integrated comparative behavior of the structural composite mortars with respect to thermal mortar sample without fiber.

Fiber percentage with respect to the mortar mass	Reduction in compressive strength	Improvement in insulating capacity (with reduction in thermal conductivity at 20 °C)
0.5% (avg. of 5 mm, 10 mm and 30 mm)	−20.27%	31.24%
1.0% (avg. of 5 mm, 10 mm and 30 mm)	−43.63%	37.51%
1.5% (avg. of 5 mm, 10 mm and 30 mm)	−56.03%	35.59%
2.0% (avg. of 5 mm, 10 mm and 30 mm)	−74.60%	38.36%

Therefore, although the introduction of fiber yields to a compressive strength and TC reduction the latter denotes an improvement in the thermal insulation of composite mortars.

Table 18
Water used with respect to total mortar mixture (mortar + fiber).

	Fiber combinations	Water used
Thermal composite mortar	0.5% fiber (30 mm, 10 mm, 5 mm)	38%
	1.0% fiber (30 mm, 10 mm, 5 mm)	43%
Structural composite mortar	0.5% fiber (30 mm, 10 mm, 5 mm)	22%
	1.0% fiber (30 mm, 10 mm, 5 mm)	26%

Table 19
Thermal composite mortars flexural test properties.

Sample type	max. deflection (d)		Strain energy (ft)		Flexural stress (σ)		Flexural strain (ε)		Moment of inertia (I)	
	Mean	Co.V	Mean	Co.V	Mean	Co.V	Mean	Co.V	Mean	Co.V
	mm	%	kNmm	%	MPa	%		%	mm^4	%
M(SAW)F0.5(5)	1.52	3.99	1.08	30.38	2.27	8.42	0.03	3.36	239551.98	2.77
M(SAW)F0.5(10)	1.14	46.75	0.65	40.38	2.06	5.55	0.02	46.34	239551.98	2.77
M(SAW)F0.5(30)	1.37	22.49	0.86	29.15	2.06	19.19	0.03	21.81	240831.12	2.56
M(SAW)F1(5)	1.00	3.47	0.47	10.36	1.49	1.87	0.02	3.97	239551.98	2.77
M(SAW)F1(10)	1.07	7.85	0.64	20.86	1.62	7.80	0.02	7.33	239551.98	2.77
M(SAW)F1(30)	1.13	2.13	0.90	3.76	1.53	1.85	0.02	2.40	239551.98	2.77

Table 20
Structural composite mortars flexural test properties.

Sample type	max. deflection (d)		Strain energy (ft)		Flexural stress (σ)		Flexural strain (ε)		Moment of inertia (I)	
	Mean	Co.V	Mean	Co.V	Mean	Co.V	Mean	Co.V	Mean	Co.V
	mm	%	kNmm	%	MPa	%		%	mm^4	%
MS(SAW)F0.5(5)	0.51	3.80	0.35	0.89	2.08	5.48	0.01	3.18	239578.03	2.41
MS(SAW)F0.5(10)	0.66	26.70	0.46	23.74	1.92	6.57	0.01	27.19	239551.98	2.77
MS(SAW)F0.5(30)	0.52	11.16	0.37	24.29	1.90	2.82	0.01	11.88	254706.76	1.79
MS(SAW)F1(5)	0.55	4.64	0.41	25.35	1.94	5.46	0.01	4.20	241233.71	1.70
MS(SAW)F1(10)	0.76	17.78	0.79	15.28	3.27	1.16	0.02	17.74	242608.61	1.64
MS(SAW)F1(30)	0.54	7.93	0.71	24.87	3.37	9.10	0.01	7.95	238673.50	0.89

Table 21
Compression tests (at SAW) – Thermal and structural mortars.

Thermal composite mortars			Structural composite mortars		
Sample type	Mean	Co.V	Sample type	Mean	Co.V
	MPa	%		MPa	%
M(SAW)F0.5(30)	7.84	6.24	MS(SAW)F0.5(30)	6.52	1.74
M(SAW)F0.5(10)	6.43	8.56	MS(SAW)F0.5(10)	6.55	6.00
M(SAW)F0.5(5)	7.31	6.59	MS(SAW)F0.5(5)	7.53	2.24
M(SAW)F1(30)	4.90	0.06	MS(SAW)F1(30)	14.31	2.92
M(SAW)F1(10)	4.97	3.92	MS(SAW)F1(10)	14.78	0.77
M(SAW)F1(5)	4.00	2.75	MS(SAW)F1(5)	7.53	6.03

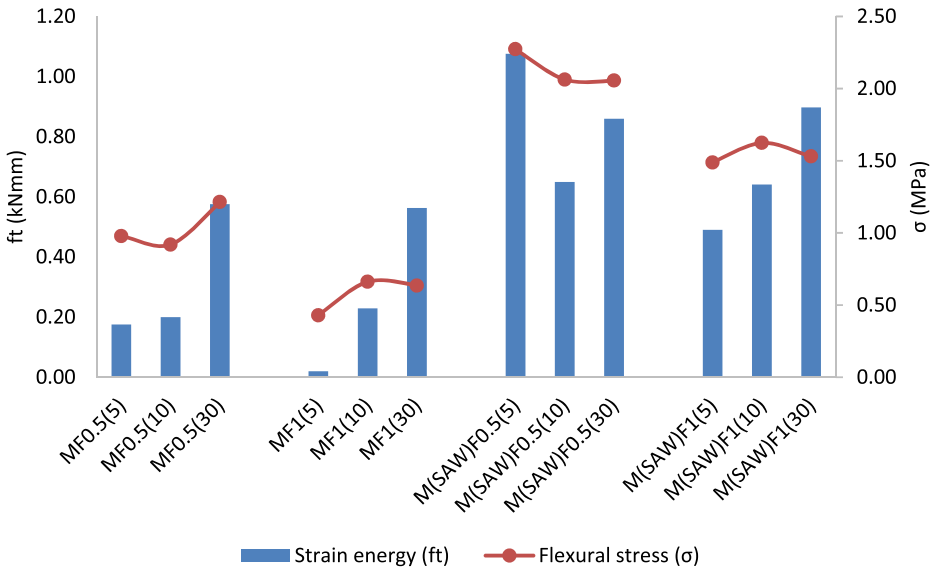

Fig. 40. Jute fiber thermal composite mortars flexural test results: SAW Vs. different percentage of water used for different fiber percentage.

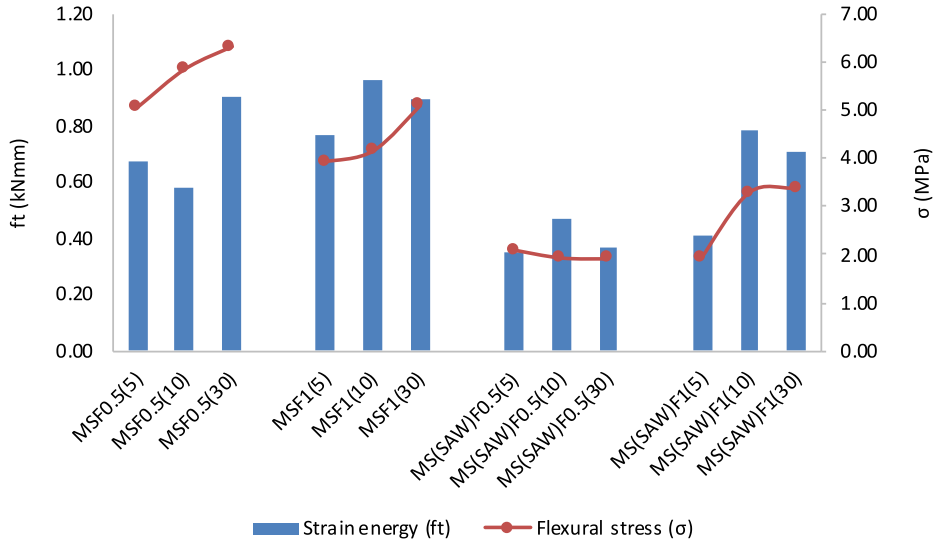

Fig. 41. Jute fiber structural composite mortars flexural test results: SAW Vs. different percentage of water used for different fiber percentage.

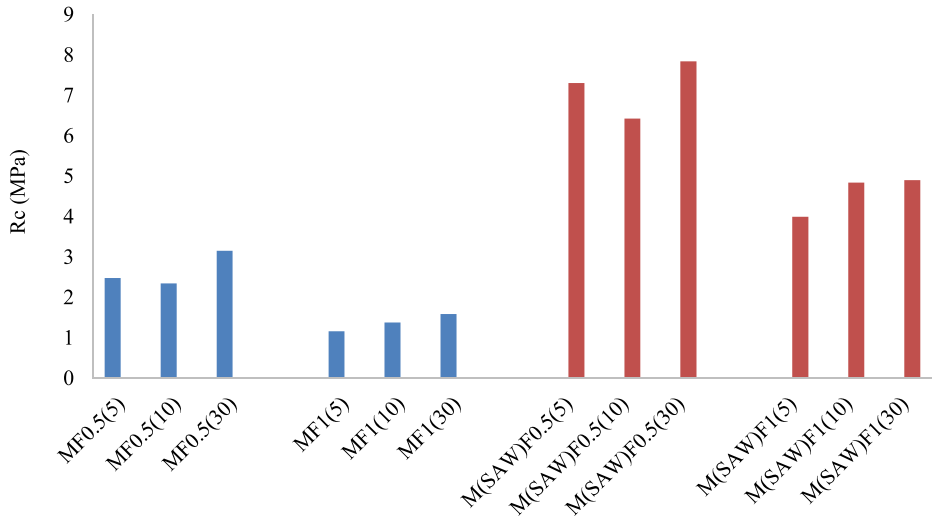

Fig. 42. Jute fiber thermal composite mortars compression test results: SAW Vs. different percentage of water used for different fiber percentage.

Fig. 47 represents the strain energy graphs for the thermal mortar without any fiber (and with pre-fabricated insulation materials or RAs) and with 6.5% recycled jute net fiber.

With the removal of the recycled aggregates from original mortar and the addition of jute fibers, the strain energy improved more than 600%, when compared with the samples without fiber and with recycled aggregates. The embodied fibers helped in absorbing and dissipating the applied load.

In addition, the thermal conductivity value (W/mK) of the oven dried jute fiber (recycled class 1 mm thread) thermal composite nRA mortar sample is 7.4% at 10 °C), 7.32% (at 20 °C) and 6.65% (at 30 °C), respectively lower than that of the oven dried normal M (No fiber) – thermal mortar reference sample, see Table 26.

Therefore, it can be concluded that by replacing and adding the recycled jute thread fibers, it is possible to improve also the insulating capacity of the composite mortars.

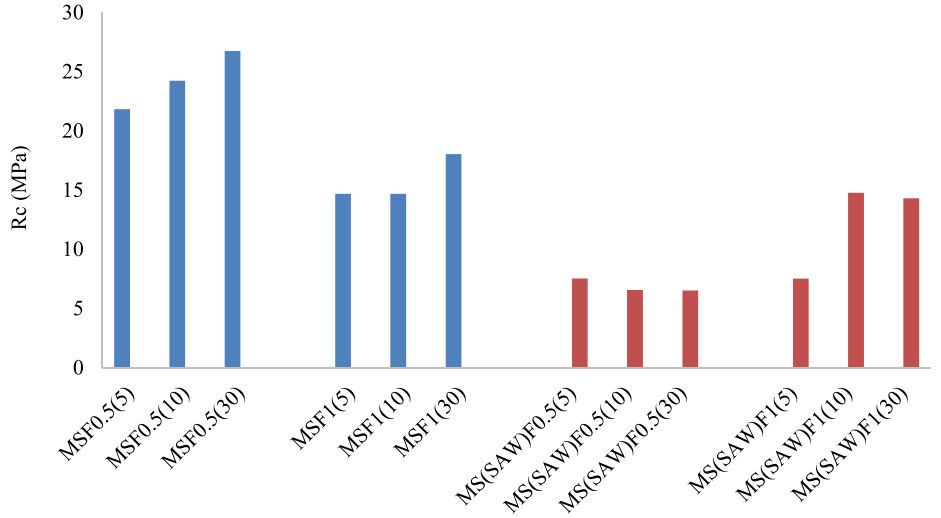

Fig. 43. Jute fiber structural composite mortars compression test results: SAW Vs. different percentage of water used for different fiber percentage.

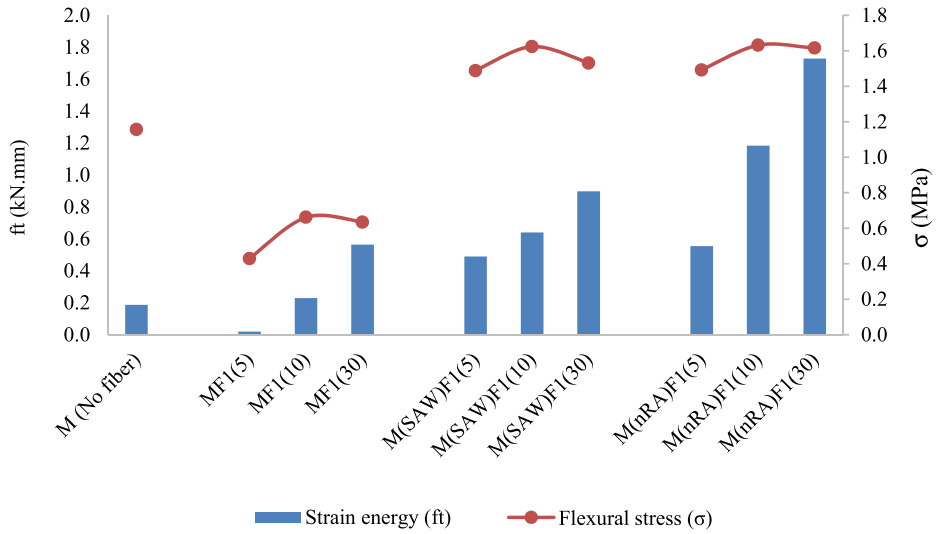

Fig. 44. Jute fiber thermal composite mortars flexural test results: nRA Vs. SAW and different percentage of water used for different fiber percentage.

Table 22
Thermal composite mortars.

Sample type	max. deflection (d)		Strain energy (ft)		Flexural stress (σ)		Flexural strain (ε)		Moment of inertia (I)	
	Mean	Co.V	Mean	Co.V	Mean	Co.V	Mean	Co.V	Mean	Co.V
	mm	%	kNmm	%	MPa	%		%	mm^4	%
M(nRA)(SAW)F1(5)	1.65	22.29	0.55	20.87	1.49	2.41	0.03	21.64	239551.98	2.77
M(nRA)(SAW)F1(10)	2.07	3.00	1.18	15.12	1.63	2.33	0.04	3.04	239551.98	2.77
M(nRA)(SAW)F1(30)	1.33	17.92	1.73	48.66	1.62	0.78	0.03	17.52	239551.98	2.77

Table 23
Compressive strength thermal composite without recycled aggregates.

Sample type	Mean	Co.V
	MPa	%
M(nRA)F1(5)	5.27	0.55
M(nRA)F1(10)	5.00	0.96
M(nRA)F1(30)	4.62	1.11

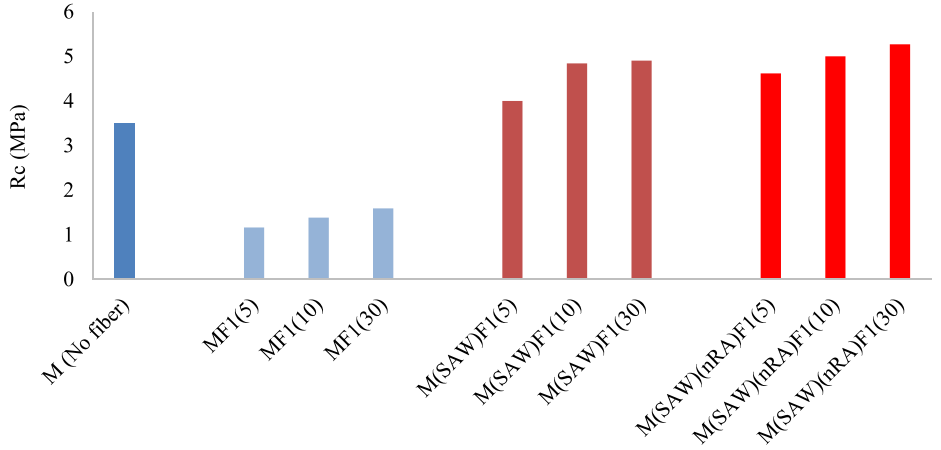

Fig. 45. Jute fiber thermal composite mortars compressive strengths: SAW Vs. different percentage of water used for different fiber percentage.

(a)

(b)

Fig. 46. (a) Flexural test and (b) compression test.

Table 24
Thermal composite mortars flexural properties.

Sample type	deflection max. (δ)		Strain energy		Flexural stress (σ)		Flexural strain (ε)		Moment of inertia (I)	
	Mean	Co.V	Mean	Co.V	Mean	Co.V	Mean	Co.V	Mean	Co.V
	mm	%	kNmm	%	MPa	%		%	mm^4	%
M(nRA)F6·5(NF) Vs M (without fiber)	0.531 / 0.603	11.540 / 9.403	1.362 / 0.186	25.756 / 29.723	0.578 / 1.156	19.152 / 6.487	0.011 / 0.013	9.623 / 9.701	244668.562 / 229219.484	8.548 / 1.051

Table 25
Thermal composite mortars compressive strength.

Sample type	Mean	Co.V
	MPa	%
M(nRA) F6·5(NF) Vs M (No fiber) – Reference Sample	19.51 / 3.50	26.54 / 9.69

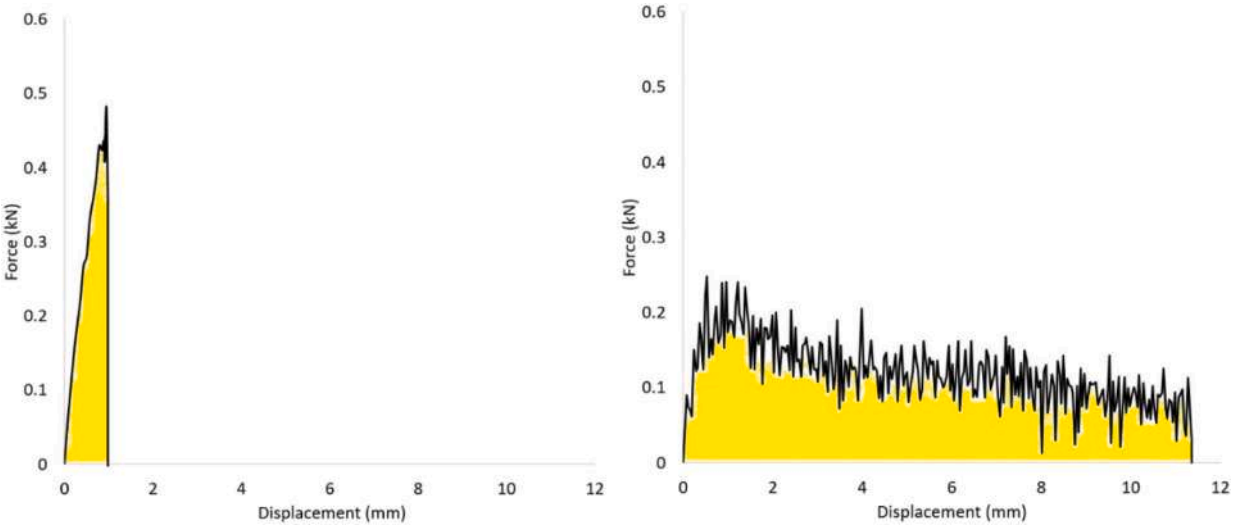

Fig. 47. Thermal mortar without fiber and with inert materials (recycled aggregates) and TM composite M(nRA)F6·5(NF) with recycled jute net-fiber and without inert materials (recycled aggregates).

Table 26
Thermal conductivity tests.

Sample type	at 10 °C	at 20 °C	at 30 °C
	λ (after oven drying at 50 °C) W/mK		
M(nRA) F6·5(NF) Vs M (with recycled aggregates and without fiber) – Reference Sample	0.213 / 0.23	0.218 / 0.236	0.225 / 0.241

4. Conclusions

Energy efficiency and structural safety represent two main goals in modern buildings. At the same time, environmental awareness requires specific attention to construction materials sustainability. For these reasons sustainable and integrated (structural and thermal) design nowadays represents an important research field.

In this paper, the effects of jute fibers in composite mortar mixes have been experimentally studied considering both the mechanical and the thermal performances.

Jute fibers composite mortars were fabricated using three different fiber lengths (5 mm,10 mm and 30 mm) and four different fiber percentages (0.5%,1%,1.5% and 2%) with respect to the mortar masses.

This study demonstrated that the addition of fibers to the mortar mixes produces an increase in porosity and a reduction of density,

consequently it leads also to a reduction of the thermal conductivity. At the same time the reduction of density produces a reduction of the flexural and compressive strength of the composite material. The results presented in Section 3.2 and 3.3 confirms these observations underlining these opposite trends in material characteristics after the fiber addition: on one side it improves the thermal behavior on the other side it reduces the mechanical performance. However, the presence of fibers tends to improve the strain energy capacity of samples yielding to flexural and compressive ductile behavior in comparison to not reinforced mortars.

Actually, the presence of fibers can be exploited with the aim to obtain the target behavior of the composite mix: on the one hand, it is possible to strongly improve the thermal insulation accepting a reduction of the mechanical properties, and, on the other hand, it is still possible to improve the strain energy capacity that can be useful in case of seismic design or in any case in which the structures should resist to extreme loads (blast, impact etc.).

Specific attention should be devoted on the amount of water in the mix design that should be calculated taking into account the presence of fibers that have a not negligible absorption capacity.

Further developments are expected in the application of these composite mortars to real structures, like masonry walls, which need specific integrated retrofitting procedures taking into account both their thermal performance and mechanical behavior.

Author statement

Arnas Majumder: Investigation, Data Curation, Writing - Original Draft, Writing - Review & Editing.

Flavio Stochino: Conceptualization, Methodology, Validation, Investigation, Resources, Writing - Original Draft, Writing - Review & Editing, Supervision, Project administration.

Andrea Frattolillo: Investigation, Methodology, Writing – Review & Editing.

Monica Valdes: Investigation, Data Curation, Writing - Review & Editing.

Geminiano Mancusi: Methodology, Validation, Writing - Review & Editing, Supervision.

Enzo Martinelli: Conceptualization, Methodology, Validation, Resources, Writing - Review & Editing, Supervision, Project administration.

Declaration of competing interest

The authors declare that they have no known competing financial interests or personal relationships that could have appeared to influence the work reported in this paper.

Data availability

Data will be made available on request.

References

[1] EUR 26157K. Pitilakis, S. Argyroudis, K. Kakderi, A. Argyroudis, H. Crowley, F. authors Taucer (Eds.), Systemic Seismic Vulnerability and Risk Analysis for Buildings, Lifeline Networks and Infrastructures Safety Gain, SYNER-G Synthetic Document, Publications Office of the European Union, Luxembourg (Luxembourg), 2013. JRC84703 available online at: https://publications.jrc.ec.europa.eu/repository/handle/JRC84703. (Accessed 1 November 2021).
[2] EN ISO 52016-1, Energy Performance of Buildings and Building Components, Comité Européen de Normalisation, Brussels, 2017.
[3] EN 1998-3, Eurocode 8, Design of Structures for Earthquake Resistance – Part 3: Assessment and Retrofitting of Buildings, Comité Européen de Normalisation, Brussels, 2005.
[4] V. UNFCCC, Paris Agreement, Adoption of the Paris Agreement, Proposal by the President, 2015, p. 282.
[5] European Commission, 2030 climate & energy framework. https://ec.europa.eu/clima/eu-action/climate-strategies-targets/2030-climate-energy-framework_en (Accessed 27 July 2022).
[6] European Commission, Nearly zero-energy buildings, available online at: https://ec.europa.eu/energy/topics/energy-efficiency/energy-efficient-buildings/nearly-zero-energy-buildings_en. (Accessed 27 July 2022).
[7] World Economic Forum, Economic Progress, Five Measures of Growth that Are Better than GDP, 2016. https://www.weforum.org/agenda/2016/04/five-measures-of-growth-that-are-better-than-gdp/. (Accessed 27 July 2022).
[8] The Global Economy.Com, Rural Population, Percent - Country Rankings, World Bank, Source, 2021. https://www.theglobaleconomy.com/rankings/rural_population_percent/. (Accessed 27 July 2022).
[9] UNDP, Housing and living conditions. https://www.teamstoendpoverty.org/wq_pages/en/visages/logement.php. (Accessed 27 July 2022).
[10] UN, Sustainable Development Goals, Department of Economic and Social Affairs, available online at: https://sdgs.un.org/goals, 2015. (Accessed 1 November 2021).
[11] F. Mistretta, F. Stochino, M. Sassu, Structural and thermal retrofitting of masonry walls: an integrated cost-analysis approach for the Italian context, Build. Environ. 155 (2019) 127–136.
[12] M. Sassu, F. Stochino, F. Mistretta, Assessment method for combine structural and energy retrofitting in masonry buildings, Buildings 7 (3) (2017) 71.
[13] L. Giresini, F. Stochino, M. Sassu, Economic vs environmental isocost and isoperformance curves for the seismic and energy improvement of buildings considering Life Cycle Assessment, Eng. Struct. 233 (2021), 111923.
[14] W.H. Khushefati, R. Demirboğa, K.Z. Farhan, Assessment of factors impacting thermal conductivity of cementitious composites A review, Cleaner Mater. (2022), 100127.
[15] B. Nagy, S.G. Nehme, D. Szagri, Thermal properties and modeling of fiber reinforced concretes, Energy Proc. 78 (2015) 2742–2747.
[16] S. Ariyanti, M. Zulkarnain, M. Lubis, Natural fibers concrete model using points launching algorithm in thermal conductivity prediction, Int. J. Multiphys. 14 (4) (2020) 347–358.
[17] M. Amran, R. Fediuk, N. Vatin, Y. Huei Lee, G. Murali, T. Ozbakkaloglu, H. Alabduljabber, Fibre-reinforced foamed concretes: a review, Materials 13 (19) (2020) 4323.
[18] B. Nagy, D. Szagri, Thermophysical behaviour of reinforced concretes, in: Proc., 6th Int. Conf. Contemporary Achievements in Civil Engineer, 2018, pp. 243–253.
[19] A. Majumder, F. Stochino, F. Fernando, E. Martinelli, Seismic and thermal retrofitting of masonry buildings with fiber reinforced composite systems: a state of the art review, Int. J. Struct. Glass Adv. Mater. Res. 5 (2021) 41–67.

[20] T. Kišiček, M. Stepinac, T. Renić, I. Hafner, L. Lulić, Strengthening of masonry walls with FRP or TRM, J. Croatian Asso. Civil Eng. 72 (2020) 937–953.
[21] V. Alecci, S. Barducci, A. D'Ambrisi, M. De Stefano, F. Focacci, R. Luciano, R. Penna, Shear capacity of masonry panels repaired with composite materials: experimental and analytical investigations, Compos. B Eng. 171 (2019) 61–69.
[22] A. Rahman, T. Ueda, In-plane shear performance of masonry walls after strengthening by two different FRPs, J. Compos. Construct. 20 (5) (2016), 04016019.
[23] A. Danish, M.A. Mosaberpanah, M.U. Salim, M. Amran, R. Fediuk, T. Ozbakkaloglu, M.F. Rashid, Utilization of recycled carbon fiber reinforced polymer in cementitious composites: a critical review, J. Build. Eng. 53 (2022), 104583.
[24] A. Kalali, M.Z. Kabir, Cyclic behavior of perforated masonry walls strengthened with glass fiber reinforced polymers, Sci. Iran. 19 (2) (2012) 151–165.
[25] S.M. Hosseini, M. Yekrangnia, A.V. Oskouei, Effect of spiral transverse bars on structural behavior of concrete shear walls reinforced with GFRP bars, J. Build. Eng. (2022), 104706.
[26] T. Stratford, G. Pascale, O. Manfroni, B. Bonfiglioli, Shear strengthening masonry panels with sheet glass-fiber reinforced polymer, J. Compos. Construct. 8 (5) (2004) 434–443.
[27] M.E. Arslan, B. Aykanat, M.A. Ayyıldız, S. Subaşı, M. Maraşlı, Effects of basalt and glass fiber composites usage for strengthening on the cyclic behavior of brick infill walls, J. Build. Eng. 52 (2022), 104405.
[28] H. Zhang, S. Ji, L. Wang, C. Jin, X. Liu, X. Li, Study on dynamic splitting tensile damage characteristics of basalt fiber reinforced concrete based on AE and DSCM, J. Build. Eng. 57 (2022), 104905.
[29] D. Zhou, Z. Lei, J. Wang, In-plane behavior of seismically damaged masonry walls repaired with external BFRP, Compos. Struct. 102 (2013) 9–19.
[30] A. Furtado, H. Rodrigues, A. Arêde, Cantilever flexural strength tests of masonry infill walls strengthened with textile-reinforced mortar, J. Build. Eng. 33 (2021), 101611.
[31] S. De Santis, G. De Canio, G. de Felice, P. Meriggi, I. Roselli, Out-of-plane seismic retrofitting of masonry walls with Textile Reinforced Mortar composites, Bull. Earthq. Eng. 17 (2019) 6265–6300.
[32] A. Dalalbashi, B. Ghiassi, D.V. Oliveira, A. Freitas, Fiber-to-mortar bond behavior in TRM composites: effect of embedded length and fiber configuration, Compos. B Eng. 152 (2018) 43–57.
[33] F. Ascione, M. Lamberti, A. Napoli, R. Realfonzo, Experimental bond behavior of Steel Reinforced Grout systems for strengthening concrete elements, Construct. Build. Mater. 232 (2020), 117105.
[34] E. Yooprasertchai, P. Wiwatrojanagul, A. Pimanmas, A use of natural sisal and jute fiber composites for seismic retrofitting of nonductile rectangular reinforced concrete columns, J. Build. Eng. 52 (2022), 104521.
[35] G. Ferrara, C. Caggegi, E. Martinelli, A. Gabor, Shear capacity of masonry walls externally strengthened using Flax-TRM composite systems: experimental tests and comparative assessment, Construct. Build. Mater. 261 (2020), 120490.
[36] A. Raji, D. Mostofinejad, M.R. Eftekhar, A novel parallel wire steel-reinforced mortar (PW-SRM) method versus textile reinforced mortar (TRM) for out-of-plane strengthening of masonry walls, J. Build. Eng. 57 (2022), 104806.
[37] M. Zhang, M. Deng, Tensile behavior of textile-reinforced composites made of highly ductile fiber-reinforced concrete and carbon textiles, J. Build. Eng. 57 (2022), 104824.
[38] C. Elanchezhian, B.V. Ramnath, G. Ramakrishnan, M. Rajendrakumar, V. Naveenkumar, M.K. Saravanakumar, Review on mechanical properties of natural fiber composites, Mater. Today Proc. 5 (1) (2018) 1785–1790.
[39] L. Francesconi, L. Pani, F. Stochino, Punching shear strength of reinforced recycled concrete slabs, Construct. Build. Mater. 127 (2016) 248–263.
[40] L. Pani, L. Francesconi, J. Rombi, F. Mistretta, M. Sassu, F. Stochino, Effect of parent concrete on the performance of recycled aggregate concrete, Sustainability 12 (22) (2020) 9399.
[41] M. Sassu, L. Giresini, E. Bonannini, M.L. Puppio, On the use of vibro-compressed units with bio-natural aggregate, Buildings 6 (3) (2016) 40.
[42] G. Martínez-Barrera, J.J. del Coz-Díaz, F.P. Álvarez-Rabanal, F. López Gayarre, M. Martínez-López, J. Cruz-Olivares, Waste tire rubber particles modified by gamma radiation and their use as modifiers of concrete, Case Stud. Constr. Mater. 12 (2020) art. no. e00321.
[43] A. Majumder, L. Canale, C.C. Mastino, A. Pacitto, A. Frattolillo, M. Dell'Isola, Thermal characterization of recycled materials for building insulation, Energies 14 (12) (2021) 3564.
[44] K. El Azhary, Y. Chihab, M. Mansour, N. Laaroussi, M. Garoum, Energy efficiency and thermal properties of the composite material clay-straw, Energy Proc. 141 (2017) 160–164.
[45] M.T. Ferrandez-García, C.E. Ferrandez-Garcia, T. Garcia-Ortuño, A. Ferrandez-Garcia, M. Ferrandez-Villena, Study of waste jute fibre panels (corchorus capsularis L.) agglomerated with Portland cement and starch, Polymers 12 (3) (2020) 599.
[46] N. de Beus, M. Carus, Natural Fibres Show Outstandingly Low CO2 Footprint Compared to Glass and Mineral Fibres – Nova-Institute Updates its Reference Study for the Automotive and Insulation Industry, PRESS RELEASE (DE/EN, 2019. https://renewable-carbon.eu/news/natural-fibres-show-outstandingly-low-co2-footprint-compared-to-glass-and-mineral-fibres/. (Accessed 27 July 2022).
[47] R. Hari, K.M. Mini, Mechanical and durability properties of sisal-Nylon 6 hybrid fibre reinforced high strength SCC, Construct. Build. Mater. 204 (2019) 479–491.
[48] T. Townsend, Natural Fibres and the World Economy July 2019, 2019. https://dnfi.org/coir/natural-fibres-and-the-world-economy-july-2019_18043/. (Accessed 27 July 2022).
[49] M.R. Bambach, Direct comparison of the structural compression characteristics of natural and synthetic fiber-epoxy composites: flax, jute, hemp, glass and carbon fibers, Fibers 8 (10) (2020) 62.
[50] M.S. Islam, S.K. Ahmed, The impacts of jute on environment: an analytical review of Bangladesh, J. Environ. Earth Sci. 5 (2012) 24–31.
[51] N. Chand, M. Fahim, Tribology of Natural Fiber Polymer Composites, Woodhead publishing, 2020.
[52] M. Zakaria, M. Ahmed, M.M. Hoque, S. Islam, Scope of using jute fiber for the reinforcement of concrete material, Textiles Clothing Sustain. 2 (1) (2017) 1–10.
[53] K.P. Garikapati, P. Sadeghian, Mechanical behavior of flax-lime concrete blocks made of waste flax shives and lime binder reinforced with jute fabric, J. Build. Eng. 29 (2020), 101187.
[54] G.M. Uddin, H. Jamshaid, A. Raza, U. Hussain, A.N. Satti, N. Hayat, S.M. Arafat, Comparative experimental investigation of natural fibers reinforced light weight concrete as thermally efficient building materials, J. Build. Eng. 31 (2020), 101411.
[55] A. Majumder, F. Stochino, I. Farina, M. Valdes, F. Fraternali, E. Martinelli, Physical and mechanical characteristics of raw jute fibers, threads and diatons, Construct. Build. Mater. 326 (2022), 126903.
[56] A. Formisano, G. Chiumiento, E. J Dessì, Laboratory tests on hydraulic lime mortar reinforced with jute fibres, Open Civ. Eng. J. 14 (1) (2020).
[57] A. Majumder, I. Farina, F. Stochino, F. Fraternali, E. Martinelli, Natural fibers reinforced mortars: composition and mechanical properties, InKey engineering materials, Trans. Tech. Pub. Ltd. 913 (2022) 149–153.
[58] A. Majumder, F. Stochino, A. Frattolillo, M. Valdes, F. Fraternali, E. Martinelli, Sustainable building material: recycled jute fiber composite mortar for thermal and structural retrofitting, in: International Conference on Computational Science and its Applications, Springer, Cham, 2022, pp. 657–669.
[59] J.M. Ferreira, C. Capela, J. Manaia, J.D. Costa, Mechanical properties of woven mat jute/epoxy composites, Mater. Res. 19 (2016) 702–710.
[60] M.A. Saleem, S. Abbas, M. Haider, Jute fiber reinforced compressed earth bricks (FR-CEB)–A sustainable solution, Pakistan J. Eng. Appl. Sci. 19 (2016) 83–90.
[61] K. Rashid, E.U. Haq, M.S. Kamran, N. Munir, A. Shahid, I. Hanif, Experimental and finite element analysis on thermal conductivity of burnt clay bricks reinforced with fibers, Construct. Build. Mater. 221 (2019) 190–199.
[62] N. Benmansour, A. Boudjemaa, G. Abdelkader, K. Abdelhak, B. Aberrahim, Thermal and mechanical performance of natural mortar reinforced with date palm fibers for use as insulating materials in building, Energy Build. 81 (2014) 98–104.
[63] S. Elfordy, F. Lucas, F. Tancret, Y. Scudeller, L. Goudet, Mechanical and thermal properties of lime and hemp concrete ('hempcrete') manufactured by a projection process, Construct. Build. Mater. 22 (2008) 2116–2123.
[64] A. Valenza, V. Fiore, A. Nicolosi, G. Rizzo, G. Scaccianoce, G. Di Bella, Effect of sheep wool fibers on thermal-insulation and mechanical properties of cement matrix, Academic J. Civil Eng. 33 (2015) 40–45.

[65] A.N. Raut, C.P. Gomez, Thermal and mechanical performance of oil palm fiber reinforced mortar utilizing palm oil fly ash as a complementary binder, Construct. Build. Mater. 126 (2016) 476–483.
[66] EN 998-1, Specification for Mortar for Masonry – Part 1: Rendering and Plastering Mortar, Comité Européen de Normalisation, Brussels, 2016.
[67] EN 1015-2, Methods of Test for Mortar for Masonry—Part 2: Bulk Sampling of Mortars and Preparation of Test Mortars, 2007.
[68] EN 1015-3 - Methods of Test for Mortar for Masonry—Part 3: Determination of Consistence of Fresh Mortar (By Flow Table), Comité Européen de Normalisation, Brussels, 2007.
[69] EN 1015-11, Methods of Test for Mortar for Masonry - Part 11: Determination of Flexural and Compressive Strength of Hardened Mortar, Comité Européen de Normalisation, Brussels, 2019.
[70] EN 13501-1; Fire Classification of Products and Building Elements - Part1: Classification Using Data from Reaction to Fire Tests, European Committee for Standardization, Brussels, Belgium, 2019.
[71] ISO 8301:1991, Thermal Insulation.Determination of Steady-State Thermal Resistance and Related Properties—Heat Flow Meter Apparatus, International Organization for Standardization, Geneva, Switzerland, 1991.
[72] EN 1946-3, Thermal Performance of Building Products and Components — Specific Criteria for the Assessment of Laboratories Measuring Heat Transfer Properties — Part 3: Measurements by the Heat Flow Meter Method, European Committee for Standardization, Brussels, Belgium, 1999.
[73] EN 12667, Thermal Performance of Building Materials and Products - Determination of Thermal Resistance by Means of Guarded Hot Plate and Heat Flow Meter Methods - Products of High and Medium Thermal Resistance, European Committee for Standardization, Brussels, Belgium, 2002.
[74] EN 12939, Thermal Performance of Building Materials and Products—Determination of Thermal Resistance by Means of the Hot Plate with Guard Ring and the Heat Flow Meter Method—Thick Products with High and Medium Thermal Resistance, European Committee for Standardization, Brussels, Belgium, 2002.